



Universidade de Aveiro

C/ Currículo Sim
Data 07/11/2018

CARACTERIZAÇÃO E MODELAÇÃO DE PROPRIEDADES TERMOFÍSICAS E DE EXCESSO DE MISTURAS EUTÉTICAS

João Miguel Lopes Costa

Dissertação de mestrado em Mestrado Integrado em Engenharia Química, apresentada ao Departamento de Química da Universidade de Aveiro, sob orientação de Dr. Pedro Jorge Marques Carvalho e coorientação de Prof. Dr. João Manuel da Costa Araújo Pereira Coutinho.



Universidade de Aveiro Departamento de Química
2018

**JOÃO MIGUEL
LOPES COSTA**

**CARACTERIZAÇÃO E MODELAÇÃO DE PROPRIEDADES
TERMOFÍSICAS E DE EXCESSO DE MISTURAS EUTÉTICAS**

**DESCRIPTION AND MODELLING OF THERMOPHYSICAL
PROPERTIES AND EXCESS OF EUTETIC MIXTURES**



Universidade de Aveiro Departamento de Química
2018

**JOÃO MIGUEL
LOPES COSTA**

**CARACTERIZAÇÃO E MODELAÇÃO DE PROPRIEDADES
TERMOFÍSICAS E DE EXCESSO DE MISTURAS
EUTÉTICAS**

**DESCRIPTION AND MODELLING OF THERMOPHYSICAL
PROPERTIES AND EXCESS OF EUTETIC MIXTURES**

Dissertação apresentada à Universidade de Aveiro para cumprimento dos requisitos necessários à obtenção do grau de Mestre em Engenharia Química, realizada sob a orientação científica do Doutor Pedro Jorge Marques Carvalho, investigador auxiliar do Departamento de Química da Universidade de Aveiro (CICECO) e co-orientação do Doutor Professor João Manuel da Costa Araújo Pereira Coutinho, Professor Catedrático do Departamento de Química da Universidade de Aveiro.

o júri
presidente

Professor Dr. Carlo Manuel Silva

Professor associado do departamento de química da Universidade de Aveiro

Professor Dr. Abel Ferreira

Professor assistente do departamento de engenharia química da Universidade de Coimbra

Professor Dr. Pedro Jorge Marques de Carvalho

Investigador auxiliar do departamento de química - CICECO (Instituto de materiais de Aveiro)

agradecimientos

First of all, I would like to express my gratitude to professor Dr. Juan Segovia and his research group TERMOCAL of the University of *Valladolid*, the way they welcomed me was heart touching.

I would also like to express an exceptional gratitude to Professor Dr. João Coutinho for receiving me in his unique research group, Path, for all these last four years and also giving me the opportunity to live a new experience working abroad.

I would be extremely ungrateful if I did not thank to all the Path members for all the support and motivation.

I would like to dedicate some words of acknowledgment to Liliana Silva that always helped me in everything that needed and to Emanuel Crespo that also gave me two helping hands every time I was stuck in soft-SAFT.

A very special thank to Dr. Pedro Carvalho for not giving up on me, for enduring my anxious behavior, for all the support and attention, for heling me at abusive off scheduled hours and for bearing my doubts in this work and in myself and for almost everything else because without him this work would not exist and I would never get the master degree in chemical engineering, i cannot promise I will be ever be good at it but he did the possible and the impossible to make it happen.

It is important for me to appreciate my friends for being my friends, for keep motivating me when I was down and for the contribute they gave to the development of this work.

At last, but definitely not least, I like to thank to my parents that sponsor my education.

palavras-chave

Solventes Eutéticos Profundos, Viscosidade, Densidade, Equilíbrio Vapor-Líquidos, Equações de Estado, soft-SAFT, Alta Pressão

resumo

Os solventes eutéticos profundos (DES), uma nova categoria de solventes, tem recentemente atraído a atenção dos investigadores devido às suas propriedades. A sua preparação fácil e baixo impacto ambiental, têm projetado estes solventes alternativos para um grande número de aplicações, nomeadamente na eletroquímica, na catálise, na síntese orgânica, em processos de dissolução e extração e na dessulfurização de combustíveis. Os DES formam-se de uma mistura eutética de um dador de ponte de hidrogénio (HBD) e um recetor de pontes de hidrogénio (HBA). Devido ao seu potencial e às enúmeras aplicações propostas, a sua caracterização físico-química torna-se extremamente relevante quando se imagina a sua introdução em processos industriais.

Este trabalho é focado na formulação das misturas eutéticas compostas por [Ch]Cl + [EG], [Ch]Cl + [Gly] e [Ch]Cl + Ureia, e na sua caracterização termofísica, nomeadamente viscosidade, densidade e pontos de ebulição numa gama de temperatura entre 283.15 K e 363.15 K e a pressões entre 0.1 e 100MPa. Os dados experimentais foram posteriormente modelados usando a equação de estado (EoS) soft-SAFT; uma EoS capaz de ter em consideração a associação existente entre os componentes do DES e que consegue descrever a sua não idealidade em fase líquida. O desenvolvimento da soft-SAFT permitiu propor um novo esquema associativo e novos parâmetros moléculares para a ureia.

keywords

Deep Eutectic Solvents, Viscosity, Density, Vapor-Liquid Equilibrium, Equation of State, soft-SAFT, High Pressure

abstract

Deep eutectic solvents (DES), a new class of solvents, have attracted the researcher's attention in the last years due to their unique and "green" properties, such as their easy formulation and environmental impact, projecting them as alternative solvents for a large number of applications, like catalysis, organic synthesis, dissolution and extraction processes, electrochemistry, material chemistry and desulfurization of fuels. DES are formed by an eutectic mixture of a hydrogen bond donor (HBD) and a hydrogen bond acceptor (HBA). Owing to their promising applications, their physicochemical characterization, aiming at their use on industrial processes, stands highly relevant.

This work focus on the formulation of eutectic mixtures, composed of [Ch]Cl + [EG], [Ch]Cl + [Gly] e [Ch]Cl + Ureia, and their thermophysical characterization, namely viscosity, density and boiling temperatures, at a wide range of temperatures (283 to 363 K) and pressures (0.05 to 100 MPa). The experimental data was further modeled using the soft-SAFT equation of state (EoS); an advance EoS able to explicitly account for the association between the DES constituents and shown to be able to describe the nonideality of the liquid phase. The soft-SAFT development allowed to propose new association schemes and molecular parameters for urea.

Contents

CONTENTS	I
LIST OF FIGURES	III
LIST OF TABLES	V
NOMENCLATURE	VI
1 INTRODUCTION	1
1.1. GENERAL CONTEXT	2
1.2. SCOPE AND OBJECTIVES.....	7
2 MODEL AND EXPERIMENTAL APPARATUS	9
2.1 SOFT-SAFT EQUATION OF STATE	10
2.2 HIGH PRESSURE DENSITY	14
2.3 HIGH PRESSURE VISCOSITY.....	16
2.4 ISOBARIC EBULLIOMETER.....	22
3 MATERIALS	25
3.1 EUTETIC SYSTEMS.....	26
3.2 SAMPLES PREPARATION.....	26
4 EXPERIMENTAL RESULTS	29
4.1 DES HIGH PRESSURE DENSITY	30
4.2 DES HIGH PRESSURE VISCOSITY.....	32
4.3 VAPOR – LIQUID EQUILIBRIUM	36
5 MODELLING	37
5.1 STRATEGY TO MODEL THE EXPERIMENTAL DATA.....	38
5.2 DENSITY MODELLING RESULTS.....	40
5.3 VISCOSITY MODELING RESULTS	43
6 CONCLUSION	48
7 FINAL REMARKS AND FUTURE WORK	49
8 REFERENCES	50
APPENDIX A – EXPERIMENTAL RESULTS	59
APPENDIX B – SOFT-SAFT EOS OPTIMIZATION	69

List of figures

Figure 1.1 Scheme that represents the difference between the eutectic point of an ideal mixture and a DES.	4
Figure 2.1 Schematic representation of the physical foundation of SAFT-type equations.	10
Figure 2.2 Schematic representation of the soft-SAFT molecular parameters.....	11
Figure 2.3 Schematic representation of the apparatus of the DMA-HPM measuring cell with the movable piston.	15
Figure 2.4 Julabo F25-HE thermostatic bath (left) and Automated pressure generator (right).....	17
Figure 2.5 Scheme that represents the coils around the fluid tube.	18
Figure 2.6 Measuring cell (left) and monitoring setup (right) composed by an Agilent 34970A thermometer, Agilent 33220A wave generator and Agilent U2352A data acquisition.	19
Figure 2.7 From the left to the right, the TRIVAC D8B vacuum pump with the cold trap TK 4-8 and the Pirani vacuum measurer.....	20
Figure 2.8 Vibrating wire viscometer with a manual pressure generator and the separation funnel from which the sample is introduced.	21
Figure 2.9 Schematic representation of the isochoric ebulliometer, figure taken from Stuckenholtz et al. ^[89]	24
Figure 4.1 Density percentage relative deviation between the experimental and literature data. Data from (left) Shahbaz et al. ^{[62],[63]} in orange and red, Mjalli et al. ^{[53],[54]} in green, grey and Yadav et al. ^{[59],[61]} in yellow and blue, (right) Leron et al. ^{[90]-[92]} ..	31
Figure 4.2 Density as function of pressure and temperature for [Ch]Cl + EG, [Ch]Cl + Gly and [Ch]Cl + Urea.	32
Figure 4.3 Viscosity as function of temperature for the systems [Ch]Cl + EG, [Ch]Cl + Gly and [Ch]Cl + Urea, at atmospheric pressure. viscosity data was obtained using the ○ SVM3000, ■ vibrating wire, ◆ falling body, ▲ from D'Agostino et al. ^[95] , ◆ from Yadav et al. ^[60] and ● from Abbott et al. ^[36]	34
Figure 4.4 Viscosity as function of pressure and temperature for the [Ch]Cl + EG, [Ch]Cl + Gly and [Ch]Cl + Urea mixtures.....	35
Figure 4.5 Boiling temperatures as function of the EG mole fraction for the mixture of Urea with ethylene glycol at 0.1 MPa and 0.07 MPa.....	36
Figure 5.1 Schematic representation of the [Ch]Cl, EG, Gly and Urea molecules with the respective interaction sites, each letter represent a different association site and the color red and blue represent the negative or positive character of the sites, respectively.	40
Figure 5.2 VLE as function of composition and pressure for the urea + EG system. The solid lines represent the soft-SAFT EoS description.	41
Figure 5.3 Density as a function of temperature and pressure for the three DES studied plus the mixture urea with ethylene glycol. The solid lines represent the soft-SAFT results.	43

Figure 5.4 Viscosity of pure ethylene glycol and glycerol in function of the temperature and for the case of ethylene glycol, in function of the pressure too. The solid lines represent the soft-SAFT prediction while the symbols represent the experimental data found in the literature	45
Figure 5.5 Viscosity as function of temperature and pressure for the three DES evaluated. The solid lines represent the soft-SAFT EoS description.	46
Figure B.1. Density as a function of temperature and pressure the choline chloride with urea, the solid lines represent the soft-SAFT prediction while the symbols are the experimental data shown above.	70
Figure B.2. Density as a function of temperature at atmospheric pressure for the mixture Urea with ethylene glycol, the solid lines represent the soft-SAFT prediction while the symbols are the experimental data shown above.	71
Figure B.3. Viscosity as a function of temperature and pressure for pure ethylene glycol, the solid lines represent the soft-SAFT prediction while the symbols are the experimental data found in the literature.	72
Figure B.4. Viscosity as a function of temperature at atmospheric pressure for pure glycerol, the solid lines represent the soft-SAFT prediction while the symbols are the experimental data found in the literature.	73
Figure B.5. Viscosity as a function of temperature at atmospheric pressure for the eutectic solvents choline chloride with ethylene glycol and with glycerol, the solid lines represent the soft-SAFT prediction while the symbols are the experimental data found in the literature.	74
Figure B.6. Boiling points of the mixture urea with ethylene glycol in function of the compositions of ethylene glycol at atmospheric pressure, the solid line as the soft-SAFT prediction while the symbols are the experimental data	75

List of tables

Table 3.1. Chemical structure, compound description, CAS number, molecular weight, mass fraction purity, and supplier of the compounds studied in this work.....	27
Table 3.2. Masses of the compounds and choline chloride mole fraction used in the preparation of the studied mixtures. The mixtures of this table were used to study the viscosity behavior.....	28
Table 3.3. Masses of the compounds and choline chloride mole fraction used in the preparation of the studied mixtures. The mixtures of this table were used to study the density behavior.	28
Table 5.1. soft-SAFT molecular and viscosity parameters gathered from literature ^{[66],[109]} and optimized in this work.	47
Table 5.2. soft-SAFT binary interaction parameters used for each system.	47
Table A 1 Density as function of pressure and temperature for the [Ch]Cl + EG deep eutectic mixture.	60
Table A 2 Density as function of pressure and temperature for the [Ch]Cl + Gly deep eutectic mixture	61
Table A 3 Density as function of pressure and temperature for the [Ch]Cl + Urea deep eutectic mixture	62
Table A 4 Density as function of pressure and temperature for the [Ch]Cl + EG mixture with 2:3 molar ratio.	63
Table A 5 Density as function of pressure and temperature for the [Ch]Cl + EG mixture with 3:7 molar ratio.	64
Table A 6 Density as function of temperature for the Urea + EG mixture at atmospheric pressure.....	65
Table A 7 Viscosity as function of temperature and pressure for pure ethylene glycol found in the literature ^[107]	Erro! Marcador não definido.
Table A 8 Viscosity as function of temperature and pressure for [Ch]Cl + EG eutectic mixture. Found in the literature ^[108]	Erro! Marcador não definido.
Table A 9 Viscosity as function of temperature for glycerol, at 0.1 MPa.	66
Table A 10 Viscosity as function of temperature and pressure for [Ch]Cl + Urea eutectic mixture.	66
Table A 11 Viscosity as function of temperature and pressure for the [Ch]Cl + Gly eutectic mixture.	67
Table A 12 Boiling temperatures as function of the composition of ethylene glycol for the Urea + EG mixture, at 0.07 MPa.....	67
Table A 13 Boiling temperatures as function of the composition of ethylene glycol for the Urea + EG mixture, at 0.1 MPa.....	68
Table B.1. Urea soft-SAFT EoS molecular parameters for the optimization attempts. .	70
Table B.2. soft-SAFT EoS viscosity parameters tested for ethylene glycol.....	71
Table B.3. soft-SAFT EoS viscosity parameters tested for glycerol.	72
Table B.4. soft-SAFT EoS viscosity parameters tested for choline chloride.	73

Table B.5. Molecular and cross-association parameters of the various attempts.....75

Nomenclature

Symbol	Description of the symbol	SI units
A	Constant of calibration	-
a	Soft-SAFT total Helmotz energy	J/mol
a^{assoc}	Soft-SAFT association term	J/mol
a^{chain}	Soft-SAFT chain association term	J/mol
a^{id}	Soft-SAFT total Helmotz energy in the ideal case	J/mol
a^{polar}	Soft-SAFT polar term	J/mol
a^{ref}	Soft-SAFT reference term	J/mol
a^{res}	Soft-SAFT residual term	J/mol
B_i	Soft-SAFT viscosity parameter of the substance i	-
B_{mixt}	Soft-SAFT viscosity parameter of the mixture	-
f	Frequency	Hz
f_0	Resonance frequency in vacuum	Hz
f_b	Half-width of the resonance curve	Hz
f_r	Resonance Frequency	Hz
k^{HB}	Soft-SAFT cross-association Volume	\AA^3
L_v	Soft-SAFT viscosity parameter	\AA
$L_{v,mixt}$	Soft-SAFT viscosity parameter of the mixture	\AA
M_W	Molar weight	$kg^{-1} \cdot mol^{-1}$
m	Soft-SAFT chain length	-
p	Pressure	Pa
p^{sat}	Saturation pressure	Pa
p^{ref}	Reference pressure	Pa
$period$	Period	s
R	Constant of the ideal gases	$J \cdot K^{-1} \cdot mol^{-1}$
r	Radius	m
T	Temperature	K

t	Time	s
T_m	Melting temperature	K
T_{ref}	Reference temperature	K
V_1	Voltage	v
V_2	Wire movement	Hz^{-1}
x	Molar fraction of a liquid	-
α	Soft-SAFT viscosity parameter	$J \cdot m^3 \cdot mol^{-1} \cdot kg^{-1}$
α_{mixt}	Soft-SAFT viscosity parameter of the mixture	$J \cdot m^3 \cdot mol^{-1} \cdot kg^{-1}$
α_{vt}	Coefficient of the thermal expansion	K^{-1}
β	Additional mass of the fluid	-
β'	Damping due to fluid viscosity	-
β_{vt}	Coefficient of the thermal compressibility	Pa^{-1}
Δ_0	Logarithmic decrement of the wire in vacuum	-
$\Delta\rho$	Density variation	$kg \cdot m^3$
ε	Soft-SAFT dispersive energy	K
ε^{HB}	Soft-SAFT cross-association energy	K
η	Viscosity	$Pa \cdot s$
Λ	Amplitude	-
σ	Diameter of a molecular sphere	\AA
ρ	Density	$kg \cdot m^3$
ρ_s	Density of the metallic falling body	$kg \cdot m^3$

1. Introduction

1.1. General Context

Horizon 2020 is the biggest EU programme that encourages research and innovation promising breakthroughs, discoveries and world-firsts by taking great ideas from the lab to the market. In the working program of the horizon 2020 programme several goals on climate policies, aiming at the reduction of the carbon and solvent emissions, are proposed. The deadline of some of these goals such as the topics “*Supporting the development of climate policies to deliver on the Paris Agreement, through Integrated Assessment Models (IAMs)*” and “*Climate change impacts in Europe*”, just to name a few, have recently expired, with some of the proposed targets not being accomplished on time. Thus new regulations are going to be proposed with more challenging and demanding targets. On the other hand, the Registration, Evaluation, Authorization and Restriction of Chemicals (REACH), a regulator that improves the protection of human health and the environment through a better and earlier identification of the intrinsic properties of chemical substances, has over the years been restricting and controlling the use of organic solvents and protocols, to treat their before the release to the environment, aiming at reducing the environmental impact. All these political decisions have inspired researchers to develop alternatives to organic solvents.

Conventional industrial organic solvents are a source of pollution with direct impact on the ozone depletion, disruption of natural ecosystems and persistent bioaccumulation. These solvents are not only an environmental concern, but people are also further exposed to them on two different ways: inhalation or cutaneous contact and, in some cases, ingestions due to unintentional or accidental exposures. The exposure to solvents have substantial neurotoxic effect to central and peripheral nervous systems which can produce severe and irreversible toxic leukoencephalopathy, more known as white matter dementia^[1].

Industries like painting^[2], construction^[3], furniture finishing^[4], metal degreasing and finishing^[5], mechanical and refrigeration systems maintenance^[6], rubber^[7], polymer^[8], textile and leather^[9] production rely on the use of organic compounds on their processes. Thus, searching for alternative solvents stands highly relevant on a near future.

In the last few decades, ionic liquids (ILs), a class of green solvents, have attracted the interest from both industry and academia. ILs consist on a salt whose ions are organized in such way that allows them to be in the liquid state bellow 100 °C. The term “ionic liquid” was coined

for the first time back in 1914 by Paul Walden^[10] for a mixture of ethylammonium nitrate, which was, at that time, proposed to be used as an alternative to nitroglycerin in explosives^[11]. Only recently, studies on ionic liquid's properties revealed the great potential of these compounds as an alternative for conventional solvents. The properties that make IL interesting as a solvent are: negligible vapor pressure, negligible flammability, thermal stability and highly solvating capacity either for polar and nonpolar compounds^{[12]–[15]}. Other applications besides solvent action have been pointed to ILs, since they have been referenced to be used in lubricants^[16], deep desulfuration of diesel fuel^[17], thermal fluids^[18], fuel cells^[19], metal finishing^[20], gas separations^[21], extractions^[22] of calcium from spiral microfluids^[23], of styrene from ethylbenzene^[24], of verbascoside from *Rehmannia* root^[25], of succinic acid from bio mass^[26] and recovery of Indium based on the combination of ionic liquid extractions with electrodeposition^[27] and liquid membranes^[28], just to name a few. Ionic liquids have been claimed as environmentally friendly since they are non-volatile (do not cause air pollution). Moreover, being composed of ions their simple combination allows one not only synthesize 10^6 different ionic liquids but to tune the solvent's properties, like density, viscosity, surface tension or even biodegradability and toxicity for microorganisms, invertebrates and vertebrates, designing them for a specific and to be “environmental friendly”^{[29][30]–[32]}.

Another alternative to conventional solvents are deep eutectic solvents (DESs). The etymology of the word *eutectic* comes from the Greek word *ευτηκτος*, which mean easy to melt. The first person to use the term *eutectic* was the British physicist Frederic Guthrie in 1884. At that time this term was used to define “*a lower temperature of liquefaction than that given by any other proportion*”. In a mixture, the interception of two solubility curves, which represents the composition at the minimum melting temperature of the mixture, is called the eutectic point, as depicted in **Figure 1.1**. DESs are eutectic mixtures of two (or more) compounds, a hydrogen-bond donor (HBD) and an hydrogen bond acceptor (HBA), able to establish strong and highly complex hydrogen bonds, that due to those interactions present a significant melting temperature depression compared to the melting temperatures expected for an ideal system.

It is important to stress that there is still some misconception around the definition of DES. They are not novel compounds or pure substances neither a new type of ionic liquid (although, most DESs reported in the literature have an ionic liquid as HBA).^[33] In fact, many mixtures are reported to be a DES but, if one evaluates their deviation to ideality, they are just common eutectic mixtures^{[33][34]}. The majority of DESs reported in literature are composed by a

quaternary ammonium halide salt, as a hydrogen bond acceptor (HBA), and a hydrogen-bond donor (HBD) that can vary from amides^[35] (like urea and its derivatives), polyols and polyalcohols (like glycerol^[36], ethylene glycol^[37] or triethylene glycol^[38]), carboxylic acids (like oxalic^[39], malonic^[40] or glutaric acid^[41]) and even sugars (like D-fructose^[42], D-glucose^[43] or xylitol^[44]).

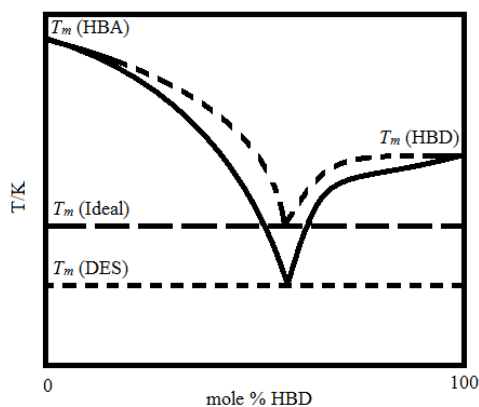


Figure 1.1 Scheme representing the difference between the eutectic point of an ideal mixture and that of a DES.

Smith et al.^[1] proposed a general formula to classify different DESs into four types, according to the nature of the DES constituents. The type I are characterized by a metal salt and an organic salt.^[45] Type II consists of a mixture of hydrated metal halide with an organic salt, this type being suitable to industrial processes because of their low price and easy shipping since it is insensitive to inherent air or moisture.

Using [Ch]Cl and a hydrogen bond donor, such as amides, carboxylic acids and alcohols one can form a type III DES^[46]. The type III DES are composed by an organic salt and a HBD making this type of DES relatively cheap solvents and characterized by a simple preparation, biodegradability and poor reactivity with water. Manipulating the hydrogen bond donors allows to attain distinctive physical properties tailoring thus the solvent for different applications, like synthesis of cellulose derivatives^[47], processing of metal oxides^[48] or removal of glycerol from biodiesel.^[49] Abbott et al.^[50] have reported the formation of mixtures of metal halides, with transition metals, and urea that form eutectic mixtures liquid at room temperature, denominating these new DES as type IV eutectics.

The use of DES as an alternative to ILs (and conventional solvents, as well) present some advantages since the selection of the HBD and HBA can lead to DES that are liquid at wider temperature ranges, less toxic solvents, cheap and biodegradable.^[29]

ILs and DES have been reported as having potential for a great number of applications. In fact, the number of articles on these classes of solvents, with an exponential increase over the last decade, is an image of the interest they have gained. However, regardless their potential and interest their thermophysical characterization is still scarce, limited to a small number of compounds or families of compounds and on a narrow window of temperatures and pressures. Furthermore, if one aims to scale-up processes, based on these systems, thermophysical properties like density, viscosity and vapor-liquid equilibria are vital for the proper process simulation and its technical and economical evaluation. In this work, eutectic mixtures and their thermophysical characterization, namely density, viscosity and boiling temperatures, as function of pressure (up to 95 MPa) and temperature (from 283 K to 373 K), will be evaluated and discussed.

Although, only density, viscosity and boiling temperature will be evaluated here, other properties like interfacial properties, such as surface tension, electroconductivity or refractive indices are highly relevant but also poorly investigated^{[51],[52]}. Experimental data on surface tensions were reported by D'Agostino et al.^[51] for the mixtures of [Ch]Cl with glycerol, ethylene glycol, urea and malonic acid at the temperature of 298.15 K. Jibril et al.^[52] reported surface tension data about mixtures of tetrabutylammonium chloride with glycerol, ethylene glycol and triethylene glycol, all of them with a composition of 1:3 of salt:HBD molar ratio and at temperature of 303.15 K. Mjalli et al.^[53] reported the same property for mixtures of tetrapropylammonium bromide with the same composition, temperatures and HBDs of Jibril et al.^[38]. At temperatures of 298.15 K, Abbott et al.^[39], Hayyan et al.^[43], Mjalli et al.^[54] reported the surface tensions of [Ch]Cl with phenylacetic acid, n-glucose and fructose, respectively. Conductivity of DES have been reported by Abbott et al.^[55] and Bandrés et al.^[56] for the choline chloride with urea at the eutectic point at temperatures of 313.15 K and 303.15 K, respectively. At 298.15 K, Abbott et al.^[36] and Bagh et al.^[57] reported conductivity values of choline chloride with glycerol and Abbott et al.^[39] and Bahadori et al.^[58] reported for choline chloride with malonic acid.

Although an increasing number of DES densities and viscosities are being reported in the literature, during the last couple of years, the range of temperatures and pressures in which these systems have been evaluated, in terms of viscosity, is limited to atmospheric pressure and temperatures up to 373 K and for pressures up to 50 MPa and 368 K for the case of density. In fact, for viscosity there is no data as function of pressure^[55] and those available are limited to a

narrow windows of temperatures^{[35],[36],[51],[59],[60]}. For viscosity, only Abbott et al.^{[35],[36],[39]}, D'Agostino et al.^[51], Yadav et al.^{[59],[60]}, Mjalli et al.^[53], Florindo et al.^[41] and Bahadori et al.^[58] reported data at temperatures ranging from 298 K to 373 K for eutectic mixtures composed of choline chloride with urea, glycerol, malonic or oxalic acid.

Densities for DES are reported for temperatures ranging from 298.15 K and 368 K and pressures up to 50 MPa. Yadav et al.^{[59],[61]}, Shahbaz et al.^{[62],[63]}, Mjalli et al.^{[53],[54]} reported density data for the eutectic mixture of choline chloride + ethylene glycol, glycerol or urea at atmospheric pressure and for temperatures ranging from 283.15 K to 368.15 K. Only Leron et al.^[64] reports density data at higher pressures (0.1 MPa to 50 MPa) and for temperatures between 298.15 K and 323.15 K for eutectic mixtures composed of [Ch]Cl + Gly, EG and Urea.

In order to evaluate these solvents real potential for industrial application their thermophysical characterization is of key importance either to dimensioning simple equipment to its phase equilibrium accurate description by a model, equation of state or correlation and further implementation in process simulators for real industrial dimensioning.

An equation of state (EoS) is a thermodynamic equation that can describe the state of the matter in a specific set of conditions; in the majority of cases by semi-empirical functional relations between temperature, pressure and volume^[65]. The availability of robust and accurate models and equations of state are vital for designing and optimizing an industrial process, so, if one aims at implementing DES at an industrial level, the development of reliable models, correlations and/or EoSs able to describe DES is of importance^[66].

Since 1662, when the Irish physicist and chemist Robert Boyle made the first expression of an equation of state, the Boyle's law, stating that the volume of a gas is inversely proportional to the pressure it is submitted. Boyle's law initiated the development of new EoSs^[65]. The classical equations of state such as, Van Der Waals was one of the first EoSs to take into account the molecular volume and interactions between substances and was the first to predict continuity of matter between vapor and liquid states. Although this EoS was not able to accurately describe the phase equilibria of some systems, the Van Der Waals EoS gave the first steps for modern cubic EoS^[65]. Based on the Van Der Waals EoS many other equations of state followed with some advantages and disadvantages over time. Two of the most used classic cubic EoS are the Peng-Robison (PRK) and the Soave Redilich Kwong (SRK). Both SRK and PRK EoS can predict relationships between pressure, temperature and phase composition in binary and

multicomponent mixtures with enough accuracy to be used in petroleum industries for the description of a wide variety of systems. Despite traditional cubic EoS are still widely used in industry, they often fail when used to describe systems of higher complexity such as those containing polar (e.g. CO₂) or associating species (e.g. water, DESs, ...) and have little to none extrapolation/predictive ability outside the range where parameters were optimized, requiring extensive amounts of experimental data^[65]. For that reason, cubic EoS have been progressively replaced by more advanced EoSs based on statistical thermodynamics concepts where such molecular effects can be explicitly accounted resulting in an increased accuracy, while providing a more realistic physical interpretation of the system. The first and utmost successful form of an engineering EoS, the Statistical Associating Fluid Theory (SAFT), was proposed by Chapman and co-workers^{[67]–[69]}. In SAFT model, a reference fluid (e.g. hard-spheres, Lennard-Jones, ...) is perturbed by different contributions, each representing a different effect on the fluids physical behavior such as the non-spherical shape of molecules, associative or polar interactions. Several SAFT variants have been proposed over the years, differing on the reference term chosen to model physical interactions while the chain and association terms (based on Wertheim's theory^{[68]–[70]}) essentially remain unchanged. SAFT-based EoS, such as PC-SAFT (Perturbed Chain SAFT)^[71], CPA EoS (Cubic Plus Association)^[72] and soft-SAFT^[73], have gathered a lot of interest over the years due to their performance. Among SAFT-based EoSs, soft-SAFT stands out has one of the most promising with a large number of works showing its capability to describe the phase equilibria of a large number of complex systems^{[74]–[78]}.

1.2. Scope and Objectives

Aiming at reducing the environmental impact imposed by the use of conventional organic solvents, while further answering the call of environment legislations and governmental expectations, the development of alternatives to organic solvents have motivated the scientific community to investigate different alternatives. Among many, deep eutectic solvent stand out as those with the highest potential. However, regardless the potential and foreseeable applications, their thermophysical characterization – key component on the successful use and development of industrial applications – are still poorly explored. Furthermore, this poor characterization also hampers the development of reliable and accurate models, correlations and/or equations of state.

This work will contribute to fulfill the lack of experimental data by determining density, viscosity and boiling temperatures, in a large range of pressures (0.07 MPa – 100 MPa) and temperatures (283.15 K and 373.15 K), of the three most common DES mixtures. Furthermore, the evaluated properties will allow to infer about the accuracy and capability of soft-SAFT EoS to model these neoteric solvents. To do it, new molecular schemes and parameters for the different DESs constituents will be proposed. Moreover, it will be coupled to the soft-SAFT EoS, the Free Volume Theory (FVT) in order allow the EoS to be able to describe transport properties.

2. Model and Experimental Apparatus

2.1 Soft-SAFT Equation of State

soft-SAFT^[79], as most SAFT-type equations, is written in terms of the system's residual Helmholtz energy (a^{res}) which is obtained as a sum of different contributions Equation (2.1).

$$a^{res} = a - a^{id} = a^{ref} + a^{chain} + a^{assoc} + a^{polar} \quad (2.1)$$

A reference term, a^{ref} , that accounts simultaneously for both the attractive and repulsive interaction between the monomers considering a Lennard-Jones (LJ) reference fluid; a^{chain} is a term accounting for the chain formation from the individual segments and an association term, a^{assoc} accounting for strong and highly directional forces such as hydrogen-bonding. Although neglected in this work, if dealing with polar molecules like CO₂, an additional contribution for polar interactions must be included (a^{polar}). In Equation (2.1), a is the total Helmholtz energy of the fluid and a^{id} is the total Helmholtz energy of an ideal gas at the same conditions of temperature, pressure and density^[80].

As it can be seen in the **Figure 2.1**, soft-SAFT represents molecules as a number of equally-sized spherical segments covalently bonded to each other forming chains that may or may not associate at specific sites (i.e. associating species present as association sites for hydrogen bonding).

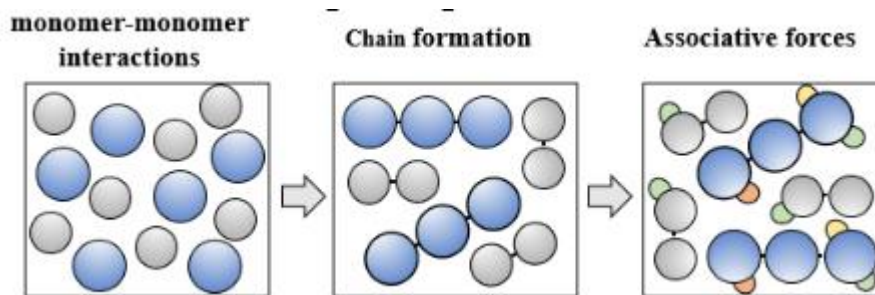


Figure 2.1 Schematic representation of the physical foundation of SAFT-type equations.

To define the LJ reference fluid, three parameters are required. The chain length parameter (m), the diameter of the monomers or groups sphere that give origin to the molecule (σ) and dispersive energy between the spheres (ϵ/k_B). In soft-SAFT, these three parameters can entirely describe a non-associating and non-polar molecule^[81].

For self-associating molecules, the association term must be enabled; an association scheme for each associating molecule must be defined specifying the number/type of association sites and interactions allowed in the system. For this, two additional parameters are required, namely the association energy (ϵ^{HB}) and volume (k^{HB}) of the association sites.

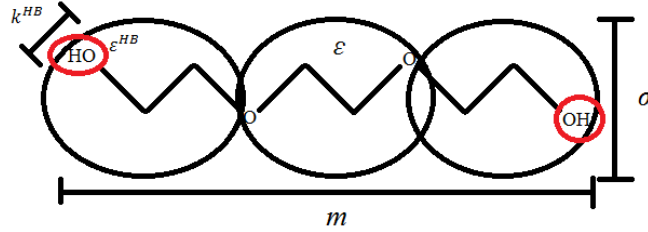


Figure 2.2 Schematic representation of the soft-SAFT molecular parameters.

The extension to mixtures is made under the van der Waals one-fluid theory using the generalized Lorentz-Berthelot (LB) mixing rules Equation (2.2) and Equation (2.3).

$$\sigma_{ij} = \eta_{ij} \cdot \left(\frac{\sigma_{ii} + \sigma_{jj}}{2} \right) \quad (2.2)$$

$$\epsilon_{ij} = \xi_{ij} \cdot \sqrt{\epsilon_{ii} \cdot \epsilon_{jj}} \quad (2.3)$$

where η_{ij} and ξ_{ij} are the size and energy correction binary parameters, fitted to binary experimental data.

When cross-association between different species is present, cross-association parameters are given by the following combining rules:

$$\epsilon_{ij}^{HB} = \sqrt{\epsilon_{ii}^{HB} \cdot \epsilon_{jj}^{HB}} \quad (2.4)$$

$$k_{ij}^{HB} = \left(\frac{\sqrt[3]{k_{ii}^{HB}} + \sqrt[3]{k_{jj}^{HB}}}{2} \right)^3 \quad (2.5)$$

One of the advantages of using SAFT-type equations is that the enhanced physical meaning of the model parameters allows to establish correlations of the non-associating molecular parameters as a function of the molecular weight for a given homologous series of compounds enabling the prediction of thermodynamic properties for compounds for which no experimental data is available. This can be done by modelling a few but representative number of members of a compounds' family and then transfer the molecular parameters to other members of the family not included in the model's parameterization or for which no experimental data is available. This feature is considered one of the greatest advantages of SAFT-type EoSs, as illustrated by Navarro et al.^[37] in a careful analysis of soft-SAFT parameters and their possible transferability. On the other hand, association parameters can remain constant when the interactions involved are similar. This meaning that the association parameters typically remain constant after the first or first two members of a series of compounds and might be transferable across different species if the same functional group is involved.

An accurate description of transport properties such as dynamic viscosity is vital for the design of several equipment used in industry due to the impact it has on the heat and mass transfer phenomena, fluid dynamics, pressure drops, etc. Different approaches have been proposed to model viscosities, ranging from empirical to highly theoretical methods. Correlations and other empirical methods are computational efficient and provide accurate results, but lack extrapolation ability and therefore, can't be applied outside the range of experimental data. On the other hand, most theoretical methods, although accurate when describing gas viscosities, fail when used to reproduce the viscosity of dense fluids.

One of the most popular approaches to model the viscosity of dense fluids is the free-volume theory (FVT) proposed by Allal et al.^{[82],[83]}. The FVT theory is based in the concept of free volume and diffusion models^{[82]-[85]}.

FVT calculates the viscosity as a sum of two terms: the diluted gas term (η_0) and the dense liquid term ($\Delta\eta$). The diluted-gas term describes the viscosity of a fluid in the very low-density region and is based on the kinetic theory of Chapman-Enskog. This term is neglected in this work given its dependency on critical properties (not available for [Ch]Cl) and the density region of interest for this work that makes of this diluted-gas term negligible if compared to the dense term.

The dense term comes from the idea that viscosity is dependent on the empty space between molecules (free-volume) through an exponential relation^[86] as depicted in Equation (2.6).

$$\Delta\eta = L_v \cdot (0.1 \cdot p + 10^{-4} \cdot \alpha \cdot \rho^2 \cdot M_w) \cdot \sqrt{\frac{10^{-3} \cdot M_w}{3 \cdot R \cdot T}} \cdot \exp^{B \cdot \left(\frac{10^{-3} \cdot p + \alpha \cdot \rho^2 \cdot M_w}{\rho \cdot R \cdot T}\right)^{\frac{3}{2}}} \quad (2.6)$$

The final equation of the dense term includes three adjustable parameters: L_v which is a length parameter related to the molecule's structure and relaxation time, B the free-volume overlap and α , which is related to the energy barrier. These parameters should be fitted to available experimental viscosity data, preferably from the pure fluid^{[86],[87]}. The Equation (2.6) also includes the pressure (p), the density (ρ), the molecular weight (M_w), the ideal gas constant (R) and the temperature (T).

As it can be observed, the viscosity calculated by the FVT model requires as an input the values of pressure, temperature and density of the system, with the accuracy of the viscosities obtained being heavily dependent on the accuracy of those values. Hence, it is important to have a reliable thermodynamic model (here soft-SAFT) that can be coupled with FVT in order to provide reliable values for such inputs.

Applying the FVT model to mixtures requires the use of mixing rules to obtain the correspondent mixture parameters. Different mixing rules have been proposed in the literature such as those of Polishuk and Yitzhak^[88], Baylaucq et al.^[89] or a simple linear mixing rule, the latter being used in this work Equations (2.7) to (2.9).

$$\alpha_{mixt} = \sum \alpha_i \cdot x_i \quad (2.7)$$

$$B_{mixt} = \sum B_i \cdot x_i \quad (2.8)$$

$$L_{v,mixt} = \sum L_{v,i} \cdot x_i \quad (2.9)$$

where x_i is the molar fraction of the compound i . It is worth highlighting that no binary parameters are fitted in the viscosity treatment of mixtures, the model was used in a predictive manner.

2.2 High Pressure Density

Vibrating tube densimeter

The oscillating U-tube (a tube in a shape of a “U”) is a technique to determine the density of liquids and gases based on the relation between the frequency of oscillation and the density (mass) of the medium. This measuring principle is based on the Mass-Spring Model. A container in a form of a hollow U-shaped glass tube is filled by the sample. This container performs an oscillation which eigenfrequency is influenced by the sample’s mass. The tube is electronically excited into undamped oscillation where the two branches of the U-tube are used as springs. The direction of the oscillation is normal to the level of the branches and only the part of the sample influences the eigenfrequency of the pendulum. The sample mass that participates in the oscillation is always the same since the volume involved in the oscillation is limited by the stationary oscillation knots at the bearing points of the oscillator. In the case of the sample’s volume overfill the oscillator beyond the bearing point, that is irrelevant for the measurement, so the oscillator is capable of measure the density of sample media that flow through the tube. In this work a DMA-HPM, coupled with a MPDS 5-unit, high pressure densimeter from Anton Paar was used to determine the density of the studied compounds in the 283.15 to 373.15 K temperature and 0.1 MPa to 95 MPa pressure ranges. The densimeter has an accuracy of 0.0001 g.cm⁻³, repeatability of 1·10⁻⁵ g.cm⁻³ and a resolution of 1·10⁻⁵ g.cm⁻³. The temperature of the measure cell was controlled with a thermo-regulated fluid (water) from Julabo, model MC, with an uncertainty of 0.01 K and stability of 0.1 K. The pressure was manipulated with a movable piston pressure generator and measured using a Kulite HEM 375 piezoresistive silicon pressure transducer, with accuracy better than 0.2% and uncertainty of 0.03 MPa. To reduce dead volumes the transducer was fixed directly in the ¼ inches stainless steel line and placed between the DMA-HPM measuring cell and the movable piston to avoid dead volumes, as depicted in **Figure 2.3**.

The densimeter was calibrated with ultra-pure water (double-distilled, passed through a reverse osmosis system, and further treated with a Milli-Q plus 185 water purification apparatus. It had a resistivity of 18.2 MΩ cm and a total organic carbon smaller than 5 mg·L⁻¹ being free of

particles greater than 0.22 mm), toluene (acquired from Sigma Aldrich, with a mass fraction purity higher than 99.8%) and dichloromethane (acquired from AnalaR NORMAPUR, with a mass fraction purity higher than 99.9%) in the (283 to 363) K, (0.1 to 100) MPa and (0.810 to 1.377) g.cm⁻³ temperature, pressure and density ranges, respectively.

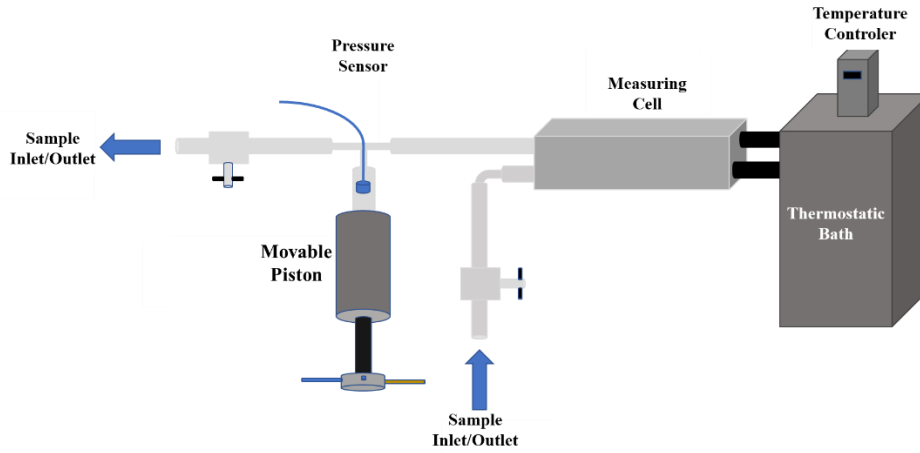


Figure 2.3 Schematic representation of the apparatus of the DMA-HPM measuring cell with the movable piston.

The polynomial suggested by the manufacturer, Equation (2.10), was adopted to calculate the density of the sample within the 0.1-100 MPa pressure, 283.15 – 363.15 K temperature and 0.810 – 1.377 g.cm⁻³ density ranges. The standard uncertainty on the density was found to be 5·10⁻⁴ g.cm⁻³[90].

$$\rho = A_1 + A_2 \cdot T + A_3 \cdot p + A_4 \cdot T^2 + A_5 \cdot p^2 + (A_6 + A_7 \cdot T + A_8 \cdot p + A_9 \cdot T^2 + A_{10} \cdot p^2) \cdot period^2 + A_{11} \cdot period^4 \quad (2.10)$$

where A_i is the polynomial coefficients, T is the temperature, p is the pressure and $period$ is the period of oscillation of the hollow tube.

The viscosity of the compounds can influence the density determination due to damping effects inside the vibrating tube, for this reason, the manufacture provided the Equation (2.11) to correct the density. However this correction was not needed since it was verified that the value of the correction was lower than the measurement uncertainty (4.84·10⁻⁴ g.cm⁻³).

$$\Delta\rho = \rho \cdot (-0.5 + 0.45 \cdot \eta^{1/2}) \cdot 10^{-4} \quad (2.11)$$

With the equipment under vacuum, the sample is injected and the temperature allowed to reach the set point. With the temperature equilibrated the pressures is changed and the the density, at a given temperature and pressure, is determined from the period of oscillation. This procedure is repeated for each intended temperature.

To clean the equipment a peristaltic pump is used to circulate, inside the equipment and through the gas/liquid line, acetone. After the solvent cleaning procedure, the solvent is initially removed by displacement using compressed air and then by applying vacuum (1 Pa) to the system.

2.3 High Pressure Viscosity

Falling Body Viscometer

A body that fall in vacuum conditions, only suffers the force of gravity. No matter the mass of the body, the acceleration that the object is subducted is always the same. However, when an object falls inside a tube filled with a substance this substance imposes an extra resistance to the falling body: the friction resistance. These two forces, gravitational and friction will be balanced at some point of the fall, and when this point is reached, the body is in a called terminal or constant velocity. This principle has been used to measure the viscosity of a substance in the falling body viscometers. In this type of equipment, the body used can be a sphere, a needle or a cylinder (body used in this study).

The operating principle of the equipment used consists on measuring of time that a cylindrical body takes to fall inside a 450 mm length tube with a diameter of 6.52 mm, at a fixed temperature and pressure. The body falls in a way that allows the fluid to ascend through a space between the cylindrical object and the wall of the tube. It is also important that the cylindrical body descends transverse its axis, otherwise the body will suffer more resistance than the expected, and the path described will be larger, leading to larger times and wrong viscosity values. The high pressure viscosity apparatus used was developed by professor Segovia's group ^{[91]-[93]} and shown to be able to determine the viscosity of a large number of fluids within the 293.15 to 393.15 K temperature, 0.1 to 150 MPa pressure and 0.27 to 1110 mPa·s viscosity ranges. The equipment was calibrated with toluene, dodecane and 1-butanol and verified, between measurements, by measuring the viscosity, at 298 K, of dioctyl sebacate and squalene.

The system that measure and control the temperature of the equipment is composed by an Agilent U2352A thermometer, four Pt100 probes to monitor the temperature, with an uncertainty of 0.05 K, and a thermostatic bath from Julabo F25-HE able to control the temperature within 235.15 to 473.15 K with an expanded uncertainty associated to resolution, uniformity and stability of 0.05 K.

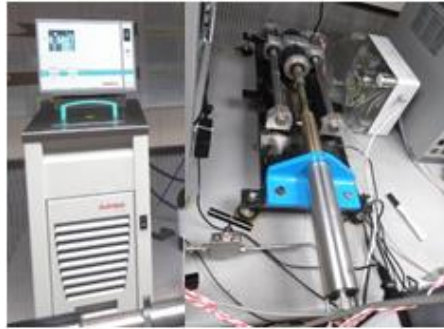


Figure 2.4 Julabo F25-HE thermostatic bath (left) and Automated pressure generator (right).

To measure the pressure a Druck DPI 104 digital manometer, with a range of (0 to 140) MPa, a resolution of 0.01 MPa, a stability of 0.05 MPa and expand uncertainty associated to the calibration of 0.05 MPa, was used. The setup to control the equipment pressure was made by an automatic triggered cylinder of variable volume from HiP, model 50-6-15 with packing of *Teflón* B-1066 and 20 cm³ controlled by a stepper motor. The results were recorded from a data Agilent U2352A data acquisition, an Agilent 34970A thermometer and an Agilent 33220A wave generator.

To measure the time that the sinker body takes to travel a defined length, a set of coils placed outside of the measuring cell (separated from each other by 50 mm) were used, as described in **Figure 2.5**. A wave generator feeds the coils with a sinusoidal signal of 2 V_{pp} (volts per pulse) and 450 Hz. When the body passes through a coil an excitation in the signal is produced allowing the operator to identify the passage of the magnetic cylindrical body at that point. By identifying the passage of the magnetic cylindrical body in two distinct positions of the cell allows one to determine the cylindrical body travel time through the sample and thus, determine its viscosity using the Equation (2.12).

Initially the apparatus were coupled with four coils. The use of four coils allows to ensure that the body is at terminal speed within the measurement zone however, the presence of four coils produced interferences on the electrical signal imposing thus noise to the measurements.

For this reason, it was opted to disconnect the two middle coils during the property determination. Nonetheless, the system's terminal speed was evaluated, using the four coils, prior to the final viscosity measurements.

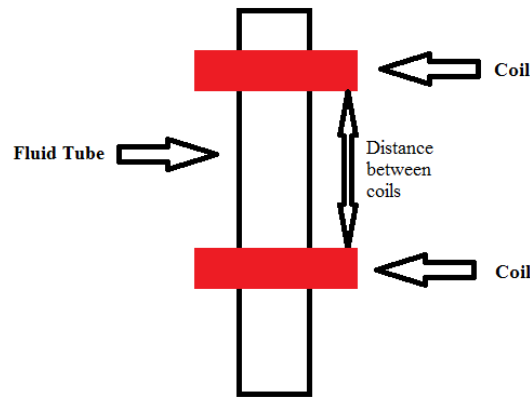


Figure 2.5 Scheme representing the coils around the measuring tube.

The measuring procedure consists in letting the thermostatic bath reach the desired temperature, set the pressure of the system, rotate the setup to place the falling body at the top of the setup and measure the time that the falling body takes to travel the defined path. The rotation of the setup is made by an automatized rotor.

On the initial runs the apparatus was positioned vertically to the ground, allowing a free fall for the falling body but, analyzing the results it was found that the cylindrical sinker descent was not smooth but colliding against the cell walls. To overcome this problem the apparatus measuring cell was tilted in 0.85 degrees aiming at achieving accurate results. The new angle of operation was nonetheless, taken into account in equipment calibration and then on the property determination.

The viscosity determination was done using Equation (2.12).

$$\eta(p, T) = \frac{t \cdot \left(1 - \frac{\rho}{\rho_s}\right)}{A \cdot \left(1 + 2 \cdot \alpha_{vt} \cdot (T - T_{ref})\right) \cdot \left(1 - 2 \cdot \beta_{vt} \cdot \frac{(p - p_{ref})}{3}\right)} \quad (2.12)$$

2. Model and Experimental Apparatus

The term time (t) is the time that the sinker body need to cross two consecutive coils, ρ is the density of the fluid at that pressure and temperature, ρ_s is the density of the metallic body. α_{vt} and β_{vt} are the coefficient of the thermal expansion and compressibility of the viscometer tube at the reference conditions of pressure p_{ref} (0.1 MPa) and temperature T_{ref} (298.15 K). The value of α_{vt} and β_{vt} are $12.8 \cdot 10^{-6} K^{-1}$ and $4.8 \cdot 10^{-6} MPa^{-1}$, respectively^[93]. A is the calibration constant, that is determine by using a well viscosity characterized substance. In the calibration the fluid tube as lightly inclined too so the calibration parameter already is affected by this modification on the equipment.

The equipment requires a sample volume of 120 mL that is introduced into the apparatus using a separation funnel connected to the inlet valve located in the top part of the measuring cell and that do not allow the entrance of the cell. Once the cell and pressure line are filled, starting from a vacuum condition, the valve is closed and the temperature and pressure allowed to reach the desired values; once the desired temperature and pressure was reached the measuring procedure was initiated.



Figure 2.6 Measuring cell (left) and monitoring setup (right) composed by an Agilent 34970A thermometer, Agilent 33220A wave generator and Agilent U2352A data acquisition.

To clean the equipment, a solvent miscible with the measuring fluid is allowed to path through the viscometer. Then, the solvent is removed by vacuum and the setup further cleaned with acetone to assure that the interior of the equipment is clean and dried after applying vacuum with a TRIVAC D8B vacuum pump coupled with a cold trap TK 4-8. The setup was considered clean when the pressure reaches $5 \cdot 10^{-2}$ mbar.

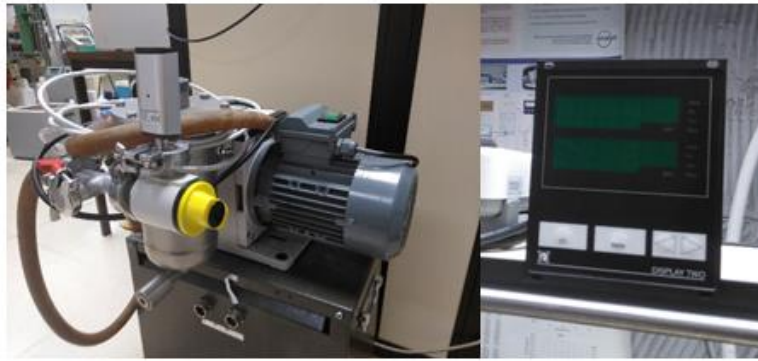


Figure 2.7 From the left to the right, the TRIVAC D8B vacuum pump with the cold trap TK 4-8 and the Pirani vacuum measurer.

Vibrating Wire Viscometer

By detailed analysis of a fluid flow around a wire, as well as the mechanical motion of the wire, it can be obtained the viscosity of the fluid. The principle used in this equipment is based in a wire that vibrates in two different oscillation modes, a forced mode and a transient mode. In the forced mode the wire vibrates in a frequency that covers its first harmonic, and the viscosity can be obtained by the width of the resonance signal. In the transient mode the wire vibrated for a short time and then stop, and the viscosity can be calculated from the decay time. The technique consists of a tungsten cylindrical wire surrounded by a fluid, of unknown viscosity, in which a constant sinusoidal current is supplied. This current together with the constant magnetic field, make the wire produce a vibration which generate a electromotive force (EMF) that is measured with a lock-in amplifier in two stages. The value of the EMF is the sum of the terms V_1 and V_2 , whose determination can be made by Equation 2.13 and 2.14, respectively. V_1 is the voltage of the impedance on the wire and V_2 is the wire movement and is proportional to the speed of the wire.

$$V_1 = a + i \cdot b + i \cdot c \cdot f \quad (2.13)$$

$$V_2 = \frac{i \cdot \Lambda \cdot f}{f_0 - (1 + \beta) \cdot f^2 + (\beta' + 2 \cdot \Delta_0) \cdot f^2 \cdot i} \quad (2.14)$$

In the Equation (2.13), f is the frequency, i is the imaginary number, a , b and c are adjustable parameters determined by regression that accounts for the electrical impedance of

the wire and the offset used in the lock-in amplifier. In Equation (2.14), Λ is the amplitude, f is the driven frequency, f_0 is the resonance frequency in vacuum, Δ_0 is the logarithmic decrement of the wire in vacuum, β ($\beta = k \cdot \frac{\rho}{\rho_s}$) is the additional mass of the fluid, β' ($\beta' = k' \cdot \frac{\rho}{\rho_s}$) is the damping due to the fluid viscosity, ρ_s is the density of the wire, k and k' are functions of $\Omega = (2 \cdot \pi \cdot f \cdot \rho \cdot R^2) / \eta$, and here ρ is the density and R is the radius of the wire. Considering that $f_0^2 = (1 + \beta) \cdot f_r^2$, and rearranging the Equation (2.14), then Equation (2.15) is obtained.

$$\eta = \frac{\pi \cdot f_r \cdot R^2 \cdot \rho}{6} \cdot \left(\frac{f_b}{f_r} \right)^2 \cdot \left(1 + \frac{\rho_s}{\rho} \right)^2 \quad (2.15)$$

where f_r is the resonance frequency and f_b is the half-width of the resonance curve.

The temperature control of the equipment is made by a thermostatic bath Hart Scientific model 6020 that has a stability of 0.01 K and can work in a range of temperatures between 20 °C and 100 °C. The measurement of the temperature of the equipment is made by a ASL F-100 and two platinum Pt100 probes inside the bath and calibrated by comparison with calibrated PRT25Ω probes. The uncertainty of the probes was determined to be 0.02 K in the 233.15 K to 503.15 K temperature range.

As in the case of the falling body viscometer, the equipment is pressurized up to 140 MPa with a cylinder of variable volume operated manually. The pressure generator cylinder, a Hip 68-5.75-10, can operate between 0.1 MPa and 140 MPa. The pressure is measured with a digital manometer General Electric DRUCK DPI 104 with a resolution of 0.01 MPa. This manometer was calibrated in Termocal Laboratory with an uncertainty of 0.02%.

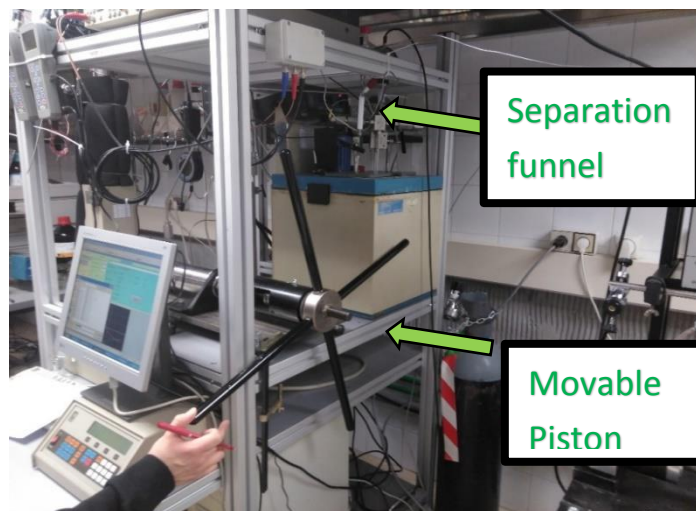


Figure 2.8 Vibrating wire viscometer with a manual pressure generator and the separation funnel from which the sample is introduced.

The setup was calibrated with reference substances, more specifically, dioctyl sebacate, squalene and dodecane showing a viscosity combined standard uncertainty of 1%.

To clean the equipment, water was used as solvent. The solvent is introduced through the separation funnel, in a similar way as the sample, and allowed to fill the setup. Then the variable volume cylinder (piston) is moved back and forward to ensure a complete and efficient cleaning procedure. These steps are performed several times until all the solvent is removed by compressed air displacement and vacuum. To ensure a complete clean setup a final cleaning procedure using acetone is performed.

SVM 3000 Anton Paar rotational Stanbinger viscometer-densimeter

The viscometer is based in a hollow tube filled with the sample and a magnetic rotor. The low density of the rotor (lighter than the sample) allows it to be centered in the liquid by buoyancy forces and the rotor is always in the same axial position due to an embedded magnet in the rotor that interact with a soft iron ring located outside the tube. The buoyancy forces create a gap between the rotor and the inside wall of the tube which force the rotor to rotate by shear stresses in the liquid. The rotation of the rotor generates a rotational magnetic field transmits a speed signal and induces eddy currents in the copper jacket that covers in tube. The speed of the rotor is influencing the eddy currents and exerts a retarding torque of the rotor. The equilibrium between the torque caused by the eddy currents and the sample cause a constant rotation of the rotor and then the viscosity of the sample can be determined. The viscometer has a temperature uncertainty of 0.02 K between 288.15 K and 378.15 K, the relative uncertainty of the measured dynamic viscosity is 1% and the uncertainty of the density is $0.0005 \text{ g}\cdot\text{cm}^{-3}$.

The equipment is cleaned passing a solvent miscible with the sample, using a peristaltic pump, then the solvent is displaced and the setup dried using dry air.

2.4 Isobaric ebulliometer

An isobaric ebulliometer able to operate at pressures ranging from 0.05 up to 0.1 MPa, was designed, assembled and tested in our laboratory. The ebulliometer, schematically presented in Fig. 2.7, is composed by three sections: a glass sample chamber container, with a total volume of 8 ml, that is placed inside of an aluminum block placed on top of a heating/stirring plate; a

glass condenser, surrounding the top section of the apparatus sample chamber, where the temperature is kept constant by means of a thermostatic bath; a liquid sampling/injection, a temperature probe and pressure line connections, done by means of vacuum tight Teflon sealed ports. Inside the ebulliometer top section a removable glass spiral increases the surface area of the reflux/condenser and the condenser, placed immediately above the sample chamber and connected to a thermostatic bath to assure a better condensation of the vapor phase generated. A Teflon-coated magnetic stirring bar, placed in the sample chamber, allows to maintain the temperature and the concentration of the sample homogeneous during the experimental procedure. The sampling/injection procedure is made by a silicone tube that passes through one of the Teflon sealed ports and connected to the sample chamber. The temperature of the liquid phase, inside the ebulliometer is measured by means of a type K thermocouple previously calibrated against a platinum resistance thermometer, SPRT100 (Fluke-Hart Scientific 1529 Chub-E4), traceable to the National Institute of Standards and Technology (NIST) with an uncertainty of less than $2 \cdot 10^{-2}$ K. The pressure is maintained constant through a vacuum line with $5 \cdot 10^{-3}$ m³ internal volume and connected to a Büchi V-700 vacuum pump and V-850 pressure monitoring and controller unit. The measuring of the pressure is made by a Baratron type capacitance Manometer, MKS model 728A with an accuracy of 0.5%. In the aluminum block there is a metallic sealed Pt100 class A temperature probe that allow the determination of the temperature difference between the sample and the block, this information helps to know if there a vapor-liquid equilibrium in the system or not.

A mixture of unknown composition is placed inside the ebulliometer and allowed to reach equilibrium, with constant and smooth boiling. Once the equilibrium is reached, the boiling temperature is measured, the liquid phase sample and the mixture composition determined through an Anton Paar Abbemat 500 Refractometer, with an uncertainty of $2 \cdot 10^{-5}$ nD, using a calibration curve previously established. The compositions have an uncertainty of $2 \cdot 10^{-5}$ g.

To clean the setup, the ebulliometer is removed from the apparatus and disconnected from the circulator thermostatic bath. Then the ebulliometer's silicon tube and the glass spiral are removed, washed and dried.

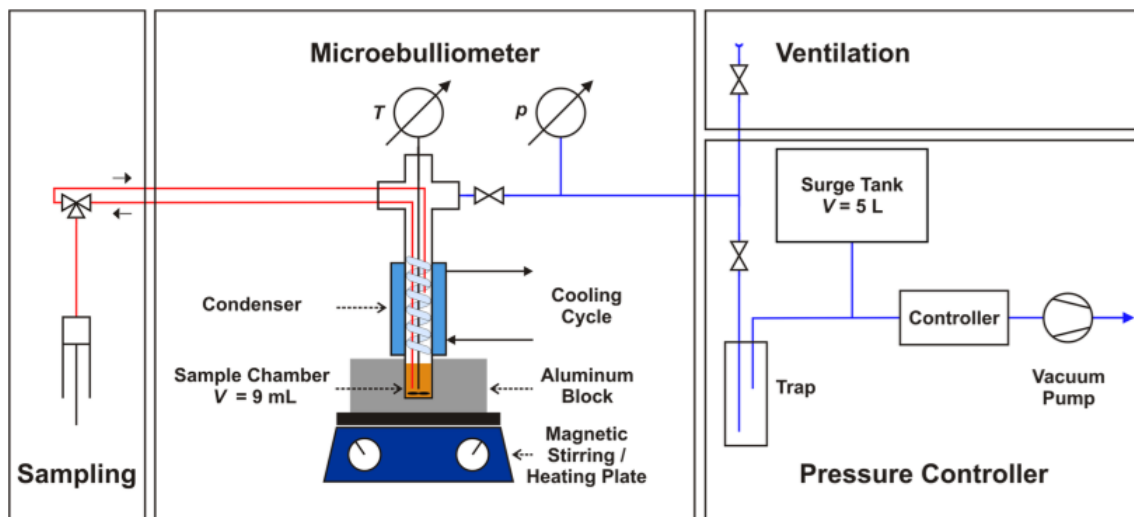


Figure 2.9 Schematic representation of the isochoric ebulliometer, figure taken from Stuckenholtz et al.^[94].

3. Materials

3.1 Eutetic Systems

Choline Chloride ([Ch]Cl), Ethylene Glycol (EG), Glycerol (Gly) and Urea were acquired from Acros Organics, Sigma Aldrich and Analar+Sigma with mass fraction purity of 98%, 99.5%, 99% and 99.5%, respectively. The compounds chemical structure, purity, supplier, and corresponding designations are presented in **Table 3.1**. It is well established that even small amounts of water and other impurities have a great impact in the compound's properties, especially on transport properties like viscosity. Therefore, with the exception of urea, that was used as received from the supplier, all the other substances were submitted to a purification methodology. Individual samples of [Ch]Cl were dried at moderate temperatures (323 K), vacuum (1 Pa) and under continuous stirring for a period never smaller than 48 hours.

Ethylene glycol and glycerol vapor pressures (18.28 and 0.04 Pa at 303 K, respectively) do not allow to adopt the purification procedure, with a vacuum of 1 Pa, adopted for the choline chloride and thus, aiming at lowering the water content the compounds were stored in a glass flask in contact with 3 Å zeolites for a minimum of 12h. The final water content, after the drying step and immediately before the mixtures preparation, was determined with a Metrohm 831 Karl Fischer coulometer (using the Hydranal–Coulomat AG from Riedel-de Haën as analyte). The average water content was found to be lower than 100 ppm.

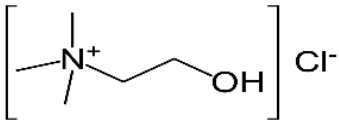
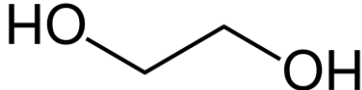
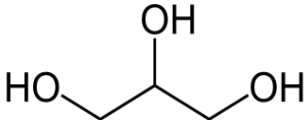
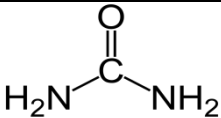
3.2 Samples Preparation

Preparation of [Ch]Cl + Urea

While urea was used directly has received from the supplier the choline chloride was purified using the abovementioned procedure. In order to avoid water absorption, from atmosphere, choline chloride was weighted using an analytical balance model ALS 220-4N from Kern with an accuracy of 0.002 g inside a dry-argon glove-box, which provides an atmosphere low in oxygen and moisture with less than 1 ppm and 2 ppm respectively. Urea is a low hygroscopic compound, so, it was weighted using a *Sartorius* analytical balance (with an uncertainty of 0.001 g) outside the glove-box. The mixture with a composition close to the eutectic point, 1 mol of [Ch]Cl to 2 mol of urea, was prepared at room temperature in a closed

Erlenmeyer containing a magnetic bar; At room temperature both compounds are solid and thus, the mixture was gradually heated in a hot plate with constant stirring, until complete homogenization, and under vacuum (1 Pa). The compounds' weight and choline chloride mole fraction of the mixture are reported in **Table 1.2** and **Table 1.3**.

Table 3.1. Chemical structure, compound description, CAS number, molecular weight, mass fraction purity, and supplier of the compounds studied in this work.

Compound	CAS	Mw	Purity (%)	Supplier	Chemical Structure
Choline Chloride	67-48-1	139.62	98%	Acros Organics	
Ethylene Glycol	107-21-1	62.07	99.5%	Sigma Aldrich	
Glycerol	56-81-5	92.09	99%	Acros Organics	
Urea	57-13-9	60.06	99.5%	Analar+Sigma	

Preparation of [Ch]Cl + EG and [Ch]Cl + Gly

The mixtures were prepared analytically with a composition close to the eutectic point, 1 mol of salt to 2 mol of HBD. The choline chloride was weighted using an analytical balance model ALS 220-4N from Kern with an accuracy of 0.002 g inside the dry-argon glove-box and the EG or the Gly were weighted using a Mottler Toledo balance with an uncertainty of 0.0001 g. The mixture was allowed to homogenize under continuous stirring. The compounds' weight and choline chloride mole fraction of the mixture are reported in **Table 1.2** and **Table 1.3**.

Table 1.2. Masses of the compounds and choline chloride mole fraction used in the preparation of the studied mixtures for the viscosity determination.

Mixture	m_1 / g	m_2 / g	x_1
[Ch]Cl (1) + Urea (2)	142.2993	126.5512	0.33
[Ch]Cl (1) + EG (2)	161.2831	138.9134	0.34
[Ch]Cl (1) + Gly (2)	122.1370	161.1139	0.33

Standard uncertainty in the masses, $u(m)$, is 0.0001 g; the combined standard uncertainty $u_c(x) = 0.01$.

Table 1.3. Masses of the compounds and choline chloride mole fraction used in the preparation of the studied mixtures for the density determination.

Mixture	m_1 / g	m_2 / g	x_1
[Ch]Cl (1) + Urea (2)	7.8831	6.8631	0.33
[Ch]Cl (1) + EG (2)	7.9402	7.0686	0.33
[Ch]Cl (1) + Gly (2)	6.4679	8.5433	0.33
[Ch]Cl (1) + EG (2)	7.9402	10.0065	0.20
[Ch]Cl (1) + EG (2)	7.8831	8.5433	0.29
EG (1) + Urea (2)	1.0452	2.5029	0.70

Standard uncertainty in the masses, $u(m)$, is 0.0001 g; the combined standard uncertainty $u_c(x) = 0$

4. Experimental results

4.1 DES High Pressure Density

The high-pressure density data was determined in the 283.15 K to 363.15 K temperature and 0.1 MPa to 95 MPa pressure ranges for the selected systems at the eutectic point. For the mixtures [Ch]Cl + EG and EG + Urea the high-pressure density was also determined for EG mole fractions of 0.6 and 0.8, for the former, and 0.7, for the later, at atmospheric pressure. The additional compositions were determined to support the development of the new soft-SAFT EoS molecular models to be discussed in a later chapter. Furthermore, and despite the property relevance the data determined here will allow to perform corrections to the viscosity determination.

Density data for the studied mixtures is scarce and those reported were determined either at atmospheric pressure or up to 50 MPa. Leron et al.^{[95],[96]} reported the density of choline chloride with urea and glycerol at pressures up to 50 MPa and in the 298.15 K to 323.15 K temperature range showing an %AD Equation (4.1) of 0.10 % and 0.23 %, respectively. At atmospheric pressure, Yadav et al.^[59] and Mjalli et al.^[54] reported densities for choline chloride with urea in the 293.15 K to 363.15 K temperature range showing an %AD of 1.1 % and -1.1 %, respectively.

$$\%AD = \sum_{i=1}^N \frac{(\rho_{Exp} - \rho_{lit})}{\rho_{lit}} \cdot 100 \quad (4.1)$$

Shahbaz et al.^[63] and Mjalli et al.^{[53],[54]} reported densities, at atmospheric pressure, and in a range of temperature of 298.15 K to 363.15 K for choline chloride with glycerol showing %AD of 2.73 %, 0.14 % and 1.18 %, respectively.

Leron et al.^[97], Yadav et al.^[61], Shahbaz et al.^{[54],[62]} and Mjalli et al. ^{[53],[54]} reported densities for [Ch]Cl with ethylene glycol, at atmospheric pressure and in the 298.15 K to 333.15 K temperature range, showing a %AD of 0.28 % and 0.27 %, 0 %, -0.04 %, -0.1 % and 1.14 %, respectively. Although small, the relative deviations may be related to the sample purity and preparation procedure since the authors did not describe the preparation methodologies neither the purification steps. **Figure 4.1** represent the relative deviation obtained between the values measured in this work and those reported in the literature^{[64],[95],[98]}.

4. Experimental Results

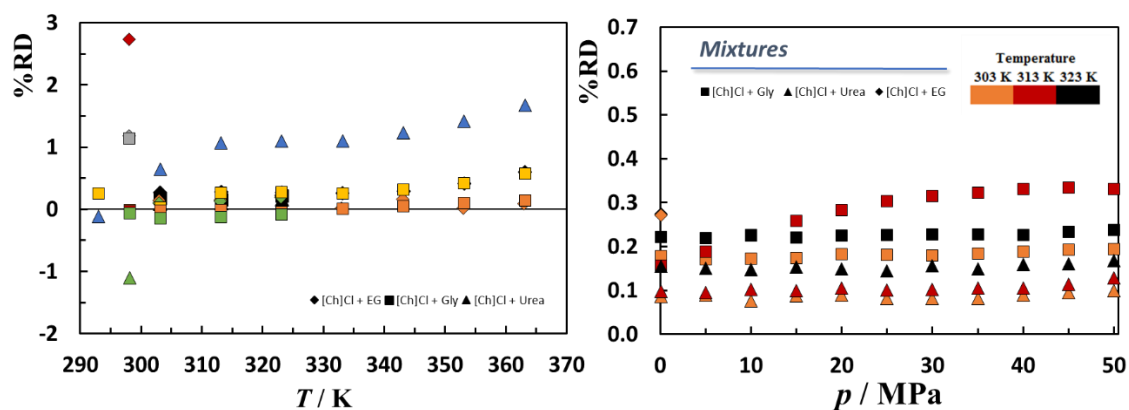


Figure 4.1 Density percentage relative deviations between the experimental and literature data. Data from (left) Shahbaz et al.^{[62],[63]} in orange and red, Mjalli et al.^{[53],[54]} in green and grey, Yadav et al.^{[59],[61]} in yellow and blue, (right) Leron et al.^{[95]–[97]}.

The high-pressure density data are depicted in the **Figure 4.2** and reported in **Table A1** to **Table A3**, in Appendix A. As can be seen, the densities ranging from 1.08 to 1.16 g·cm⁻³, 1.15 to 1.23 g·cm⁻³ and 1.15 to 1.23 g·cm⁻³ were obtained for the eutectic mixtures composed of [Ch]Cl + EG, [Ch]Cl + Gly and [Ch]Cl + Urea, respectively. Observing the density data, it can be seen that the mixture [Ch]Cl + Urea is the one that has the highest density and [Ch]Cl + EG has the lowest, these results, as expected, follow the increase of the mixture molar volume, known to be an additive property, with ethylene glycol (1.11 g·cm⁻³), glycerol (1.26 g·cm⁻³) and urea (1.32 g·cm⁻³).

4. Experimental Results

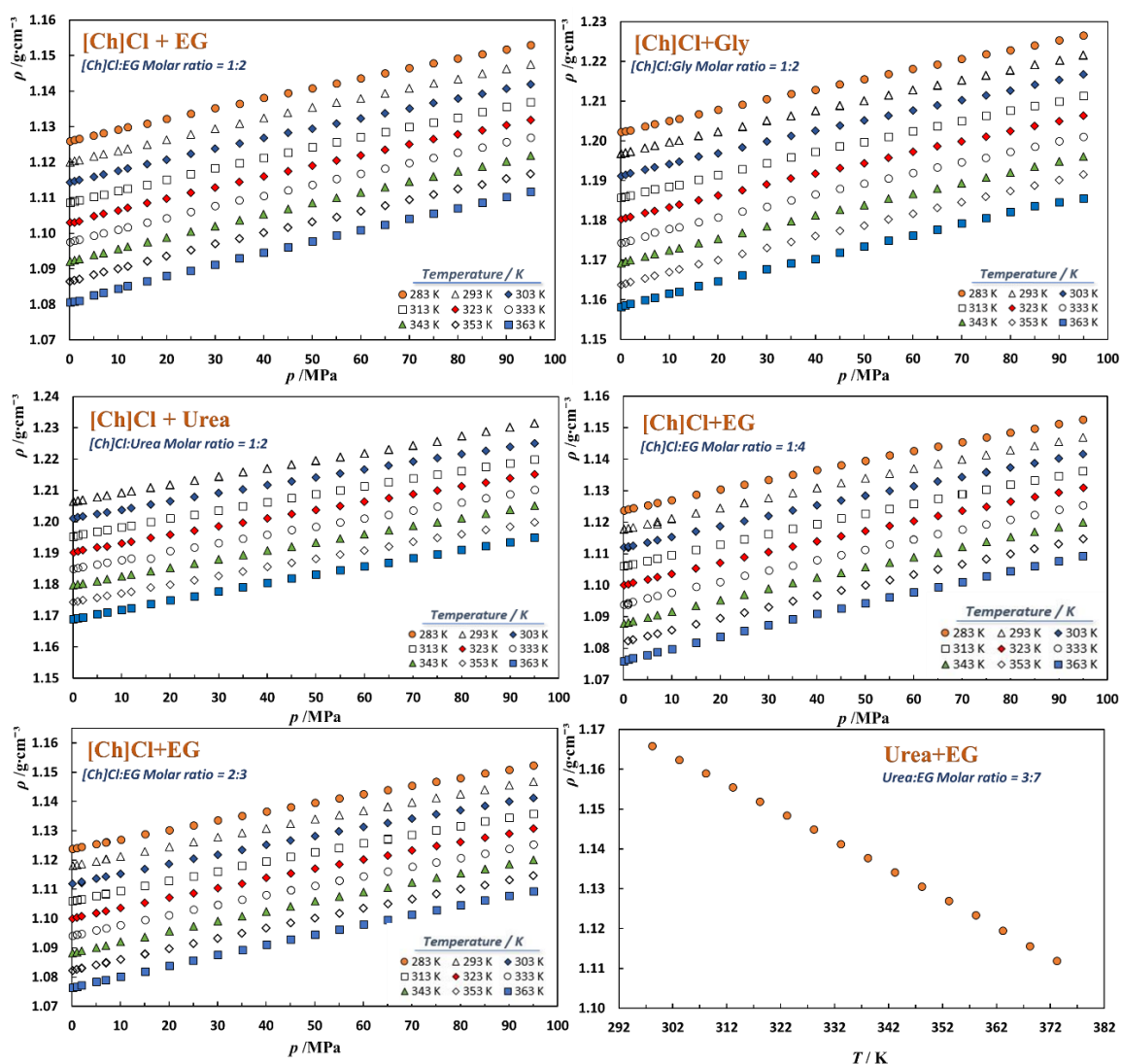


Figure 4.2. Density as function of pressure and temperature for [Ch]Cl + EG, [Ch]Cl + Gly and [Ch]Cl + Urea.

4.2 DES High Pressure Viscosity

High pressure viscosity was evaluated in the 313.15 K to 373.15 K temperature and 0.1 MPa to 100 MPa pressure ranges. As reported in the “

Model and Experimental Apparatus” section two techniques and methodologies were available for the high-pressure viscosity determination. In an initial approach both methods were evaluated by measuring the viscosity of the [Ch]Cl + EG eutectic mixture, at atmospheric

pressure, and compared against the data obtained using the Anton Paar SVM3000 viscometer that has shown to be adequate to determine accurately the viscosity of these family of compounds^{[35],[99],[100]}. As depicted in **Figure 4.3**, the viscosity obtained was concordant among each the different techniques, with %AD of 2.98 % and 1.01 % for the falling body and vibrating wire methodologies, respectively. Unfortunately, the vibrating wire equipment presented some difficulties in measuring the viscosity of the different samples due to a malfunction that made it unable to measure at viscosity higher than 15 mPa·s. Therefore, the use of the vibrating wire equipment was abandoned.

DES viscosity data is scarce in the literature and to the best of our knowledge only data from D'Agostino et al.^[100], Yadav et al.^[60] and Harris et al.^[51] at atmospheric pressure, is available for the studied systems. As depicted in **Figure 4.3**, the data obtained in this study presents large deviations against that reported by D'Agostino et al.^[100]. Furthermore, for the system [Ch]Cl + EG the viscosity behavior as function of temperature presents a distinct slope as that determined here through three different methodologies. Data from Yadav et al.^[60] and Abbott et al.^[36] are concordant among each other but with large deviations against ours. Although, the authors do not mention the compounds purity and water content it stands difficult to argue against the observed discrepancies but one can argue that the slightly different final compositions of the eutectic mixtures may lead to the deviations found against the data reported by Yadav et al.^[60] and Abbott et al.^[36].

The high-pressure viscosity, as function of temperature and pressure, is depicted in **Figure 4.4** and reported in **Erro! A origem da referência não foi encontrada.** to **Table A9** for all the mixtures evaluated. As depicted in **Figure 4.3** and **Figure 4.4** temperature has a greater impact on this property than pressure. At higher temperatures, the molecules of the mixtures are submitted at a higher energy and it is easier for them to move around and interact with other molecules, what helps them to flow with less difficulty and that is the reason that explained the decrease of the mixtures' viscosity with temperature^[101]. The increase of pressure decreases the free volume of liquids, at isothermal conditions and moderate pressures, leading to an increase of the viscosity but less pronounced than that imposed by the temperature effect^[102].

4. Experimental Results

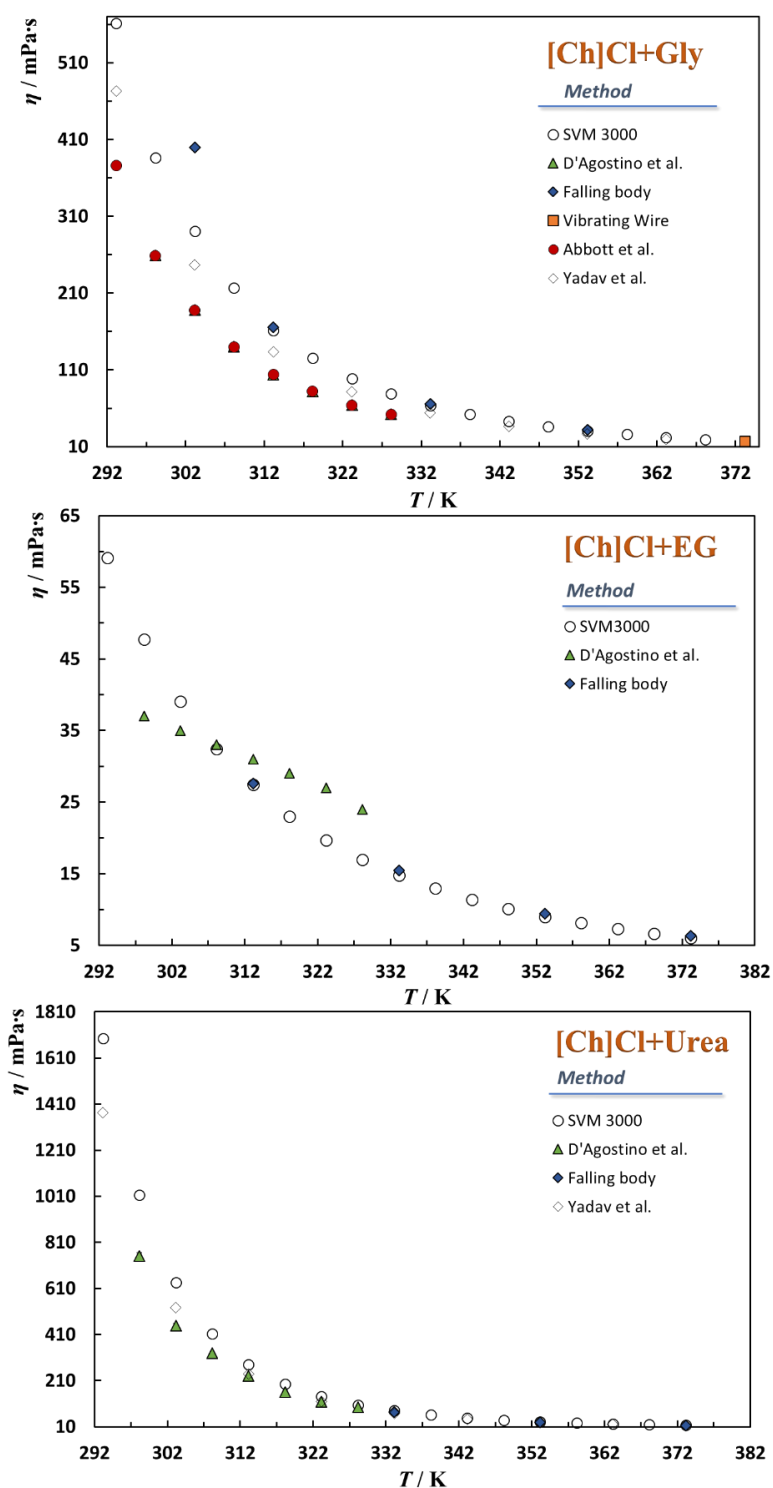


Figure 4.3 Viscosity as function of temperature for the systems [Ch]Cl + EG, [Ch]Cl + Gly and [Ch]Cl + Urea, at atmospheric pressure. viscosity data was obtained using the \circ SVM3000, \blacksquare vibrating wire, \blacklozenge falling body, \blacktriangle from D'Agostino et al.^[100], \blacklozenge from Yadav et al.^[60] and \bullet from Abbott et al.^[36].

4. Experimental Results

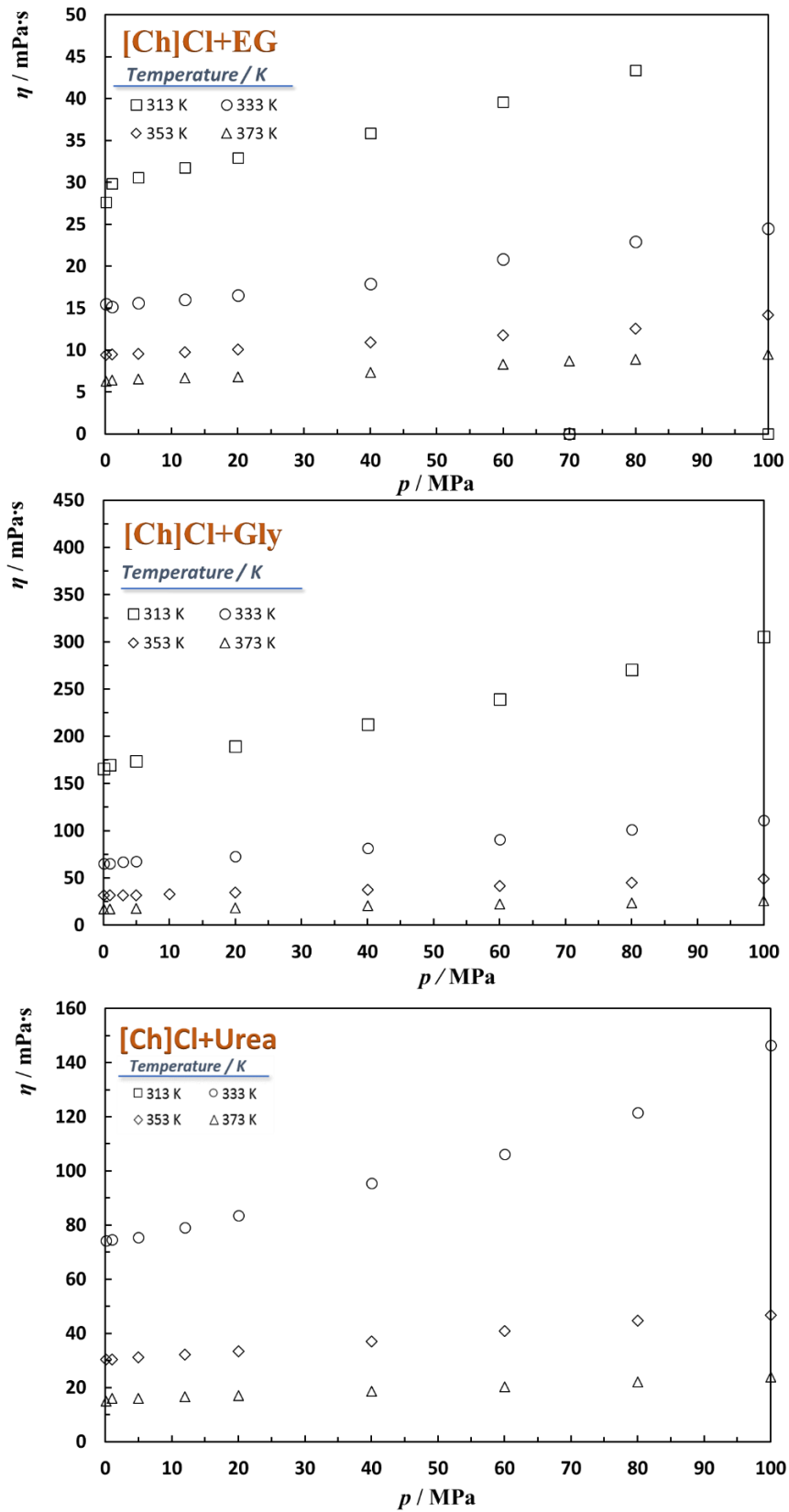


Figure 4.4 Viscosity as function of pressure and temperature for the [Ch]Cl + EG, [Ch]Cl + Gly and [Ch]Cl + Urea mixtures.

4.3 Vapor – Liquid Equilibrium

To model the proposed solvents with soft-SAFT EoS it is necessary to determine the molecular parameters of the pure components that integrate the proposed mixtures. The parameters for ethylene glycol, glycerol and [Ch]Cl have been reported by Crespo et al.^{[66],[103]}. In the ideal case, it would be recommended to use only pure compound property data to regress the molecular parameters, since the governing interactions in a pure substance are different from the interactions of that substance in a mixture. However, given the high melting temperature of urea (405 K) there are no vapor pressures and liquid densities of the pure compound thus, data from mixtures needs to be considered. In the literature there are VLE for mixtures of urea with water, reported by Azevedo et al.^[104] Perman et al.^[105] and Hou et al.^[106], but it was decided not to use data of aqueous mixtures given the unique behavior of many compounds when present in an aqueous solution. Moreover, temperature-dependent binary parameters may need to be simultaneously fitted in order to achieve quantitative agreement with the experimental data as observed with Zubeir et al.^[107] using PC-SAFT to model [Ch]Cl. For this reason, the vapor-liquid equilibrium of the binary mixture of urea + EG was measured in this work at 0.07 and 0.1 MPa and the experimental data used to determine the urea molecular parameters following a procedure explained in detail on the next chapter.

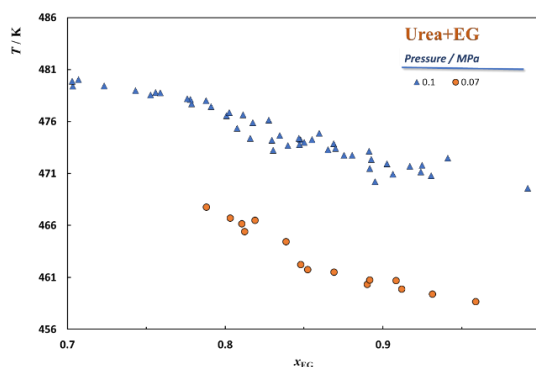


Figure 4.5 Boiling temperatures as function of the EG mole fraction for the mixture of Urea with ethylene glycol at 0.1 MPa and 0.07 MPa.

To the best of our knowledge, there is no published data available in the literature on vapor–liquid equilibrium for this mixture. As it can be seen in the **Figure 4.5**, the boiling temperature increases exponentially as the Urea mole fraction increases, going from the EG boiling temperature to that of urea.

5. Modelling

5.1 Strategy to model the experimental data

Being soft-SAFT a molecular-based EoS, the adequate selection of a reliable coarse-grained model, capable of representing the basic physical features of the compounds, stand as highly relevant for the accurate description of the systems phase equilibria and thermophysical properties. Soft-SAFT EoS relies on the pre-selection of a molecular model for the pure compounds, and determination of the correspondent molecular parameters as discussed in section 2.1.

From the compounds investigated in this work, only EG has been extensively studied with soft-SAFT. Pedrosa et al.^[90] used soft-SAFT for the systematic study of glycol oligomers (EG to TeEG). A 2B association scheme (one positive (A) and one negative (B) association sites with AB interactions being allowed) was assigned to the different glycols and the parameters were regressed from experimental VLE data for the pure compounds with the association parameters remaining constant for the different glycol oligomers. The molecular models developed in this work were used to successfully describe different binary mixtures composed of glycols with either nitrogen, methane, benzene and CO₂ using a binary interaction parameter. Later, Crespo et al.^[66] found that the parameters proposed by Pedrosa et al.^[90] failed when used to describe the second-order derivative properties such as the isothermal compressibility and isobaric thermal expansion of the pure glycols. In their work a new molecular model for glycol oligomers where glycols were modelled with two association sites (A') of dual nature and A'A' interactions being allowed was developed (further extending the study up to hexaethylene glycol) and shown to provide reliable results at a larger pressure range (up to 95MPa). Nevertheless, given the controversy about the use of dual nature sites (like those suggested by Crespo et al.) the molecular model and parameters for EG proposed by Pedrosa et al.^[90] were used throughout this work.

In a more recent work, Crespo et al. reported coarse-grained molecular models for [Ch]Cl and glycerol. For glycerol, the 2B association scheme was considered and the correspondent molecular parameters obtained by fitting to the experimental vapor pressures and liquid densities of the pure fluid. Concerning [Ch]Cl, the standard methodology can't be applied given the high melting temperature of this salt (approximately 597K) as no thermophysical properties are available for the pure component.

In the absence of pure compound properties, Crespo et al.^[103] suggested the use of selected binary mixture data, preferably corresponding to a typical DES in the parameterization procedure. Hence, these binary mixtures should be composed of the target compound and a second compound already fully characterized with soft-SAFT in order to obtain the unknown molecular parameters. Furthermore, given that the new molecular parameters obtained in this way may be influenced by the interactions characterizing the mixture, masking the physical features of the pure compound, the use of mixtures in which one can, up to a certain extent, know the kind of interactions established in the system may reduce this impact. Therefore, experimental data from very diluted aqueous solutions although commonly reported in literature should be avoided given the lower concentration of the target compound and the fact that the interactions governing the system are much different than those observed in a DES. Moreover, temperature-dependent binary interaction parameters are frequently required in order to model aqueous solutions of [Ch]Cl^[107] increasing the number of parameters to be regressed from experimental data and deteriorating the physical meaning of the parameters obtained.

Crespo et al.^[103] modelled [Ch]Cl as LJ chains with five associating sites, “A” and “B” mimicking the hydroxyl group, a pair “C” and “D” sites mimicking the cation and anion interactions as commonly done for salts and ionic liquids and an additional “C” site that represents the hydrogen bond acceptor character of the methyl groups that were found to enter important doubly-ionic hydrogen bonds within DESs systems^[108]. The corresponding molecular parameters and a state-independent binary interaction parameter were then regressed from experimental high-pressure liquid densities (measured in this work) and vapor-liquid equilibria of [Ch]Cl+EG (1:2) DES.

A similar methodology is followed in this work to obtain the molecular model for urea. Therefore, urea was modeled as LJ chains with three associating sites, “G” and “H” mimicking the hydrogen atoms of the hydroxyl group and the lone pair of electrons in nitrogen, respectively. The “I” site mimicking the two lone pairs of electrons on the oxygen.

The association parameters can be transferred from chemical family groups. For choline chloride, the parameters for “A” and “B” sites were transferred from alkan-1-ol family reported by Dr. Pàmies PhD thesis, the cation-anion interactions “C” and “D” sites were transferred from the modeling of the symmetrical tetraalkylammonium chlorides reported by Lloret et al.^[109].

For easier visualization the big grey and the red circles in the molecular structures represented in the **Figure 5.1** are the chemical groups which are associated with the association parameters and the molecular model used for the studied compounds.

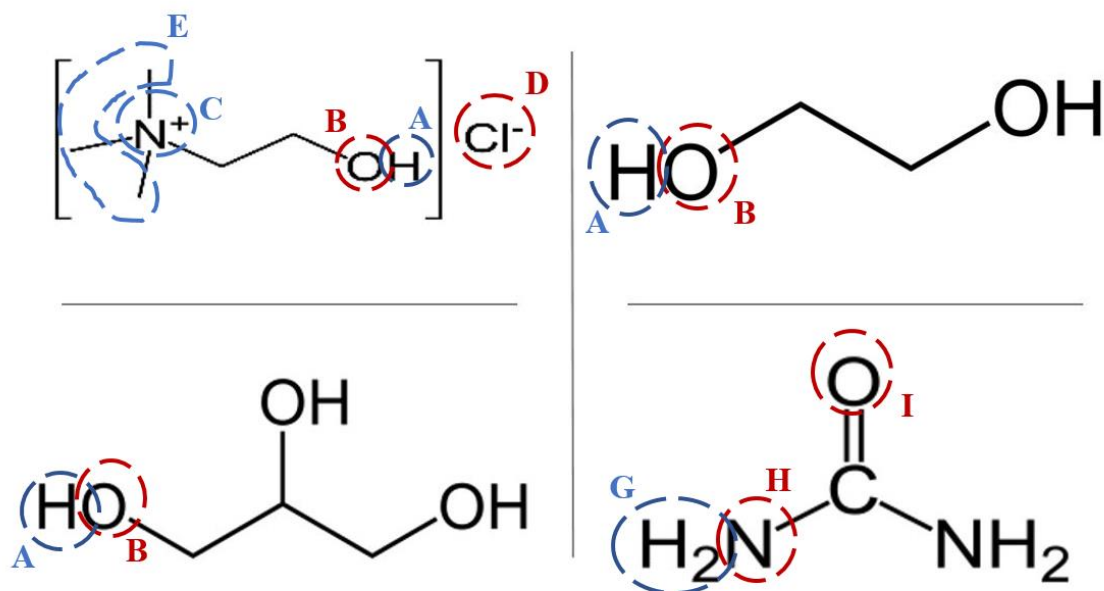


Figure 5.1 Schematic representation of the [Ch]Cl, EG, Gly and Urea molecules with the respective interaction sites, each letter represent a different association site and the colors red and blue represent the negative or positive character of the sites, respectively.

5.2 Density modelling results

The density data measured here, as function of temperature (from 283 K to 263 K) and pressure (from 0.1 MPa to 95 MPa), for the EG + [Ch]Cl, glycerol + [Ch]Cl, urea + [Ch]Cl and ethylene glycol + Urea mixtures, were used to determine the [Ch]Cl and Urea molecular parameters. For urea, additional data for the urea + EG vapor-liquid equilibria was used to support the molecular parameters optimization, as depicted in **Figure 1.2**. For the optimization of soft-SAFT molecular parameters, its density data allows to adjust and infer on the size related parameters, such as length parameter (m), diameter parameter (σ) and volume cross-association parameter (k^{HB}), while VLE data or other energy related properties enhance the validity of the energy related parameters, like dispersive energy (ϵ/k_B) and energy association parameter (ϵ^{HB}/k_B).

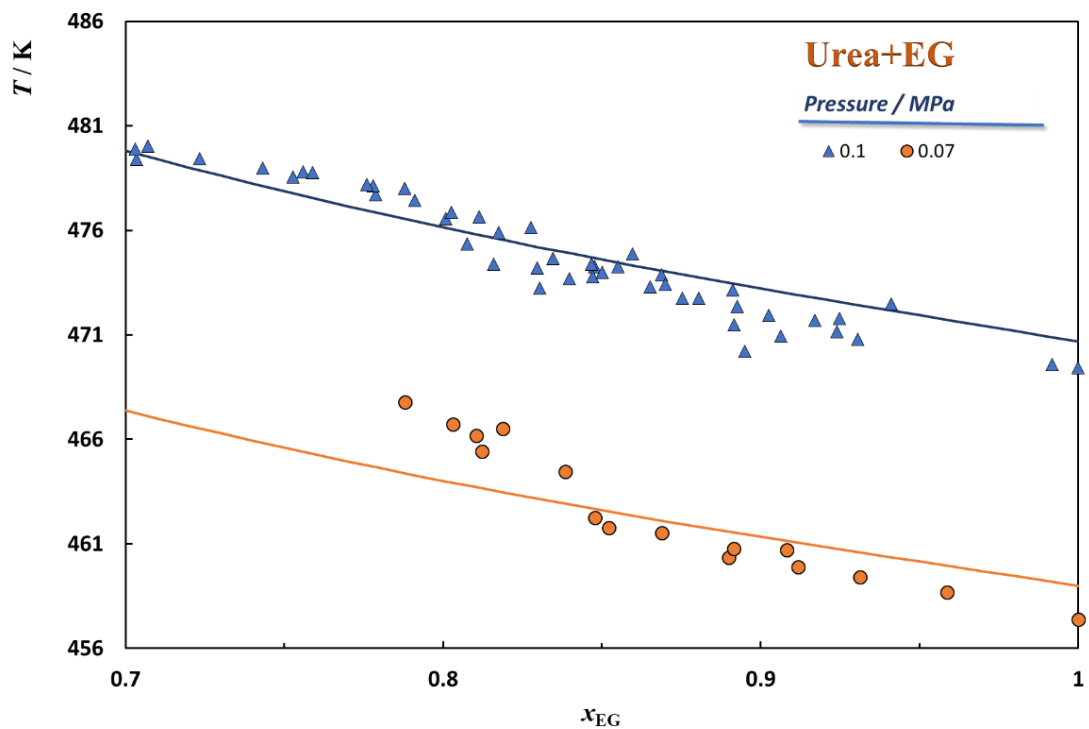


Figure 1.2 VLE as function of composition and pressure for the urea + EG system. The solid lines represent the soft-SAFT EoS description.

As depicted in **Figure 1.2**, soft-SAFT is able to describe correctly the VLE data obtained for the systems but over predicts the boiling temperature of the pure EG by two degrees. Furthermore, for urea mole fractions higher than 0.2 soft-SAFT under-predicts the boiling temperatures for 0.07 MPa. The deviation of the model with the pure EG boiling point are due to a mistake made in the optimization of the molecular parameters in a previous works.

To optimize the parameters a Matlab™ optimization routine was developed. In this routine, a matrix representing the association scheme of the substance/mixture is created and, using initial estimates for the molecular parameters, the desired property (VLE and / or density, in this work) is calculated at the given conditions of temperature, pressure or even composition, for a different combination of molecular parameters in each iteration. In each one, the routine determines the deviation between the soft-SAFT results and the experimental values and keeps running until it finds a combination of molecular parameters that minimizes the deviation to its minimum. However, the optimization was not achieved in the first attempt. In most times, the routine converged to a combination of molecular parameters that still did not describe the data accurately enough and/or the resulting parameters did not have physical significance. To help the routine converge to parameters that described the data with physical meaning, the routine

was modified to allow for fixing one or more parameters fixed. The parameters of urea were adjusted to the VLE and density data of the EG + urea mixture and then, it was confirmed if the parameters adjusted could describe the density data of the [Ch]Cl + urea mixture. The number of attempts to determine the molecular parameters of urea can be found in **Table B.1**, in Appendix B.

The chain length parameter (m) obtained is around three which makes sense considering that urea may be divided in three major 'groups' – two NH_2 groups and one carbonyl group $\text{C}=\text{O}$. Furthermore, the product $m\sigma^3$ which may be related to the volume occupied by molecules and the dispersive energy parameter (ϵ/k_B) were in good agreement with those of Held et al.^[110] with PC-SAFT. The association parameters for the chemical group NH_2 were taken from the work of Pereira et al.^[111] who successfully modelled different amines using the soft-SAFT EoS. The optimized value of the cross-association energy it was used the Matlab™ routine that gave a value of 436.17 K for the ketone group of urea. The cross-association volume were assumed equal to the association volume parameter of the NH_2 group. The attempts made to adjust the parameters of urea can be seen in **Figure B.6**, in Appendix B.

Once the molecular models for all the studied compounds are available, they can be used for the prediction of the high-pressure liquid density measured in this work. These results are shown in **Figure 1.3**.

The results of the soft-SAFT predictions for density can be considered accurate taking into account the large temperature and pressure ranges of the experimental data. In all systems, it can be seen that the absolute deviation between the experimental data and the prediction do not exceed the $0.01 \text{ g}\cdot\text{cm}^{-3}$, which when converted to units used in industrial processes is equivalent to $10 \text{ kg}\cdot\text{m}^{-3}$, which do not represent a huge deviation in processes that deal with hundreds or thousands of cubic meters per hour. So, it is possible to say that soft-SAFT is suitable for the designing of industrial processes that use the studied mixtures.

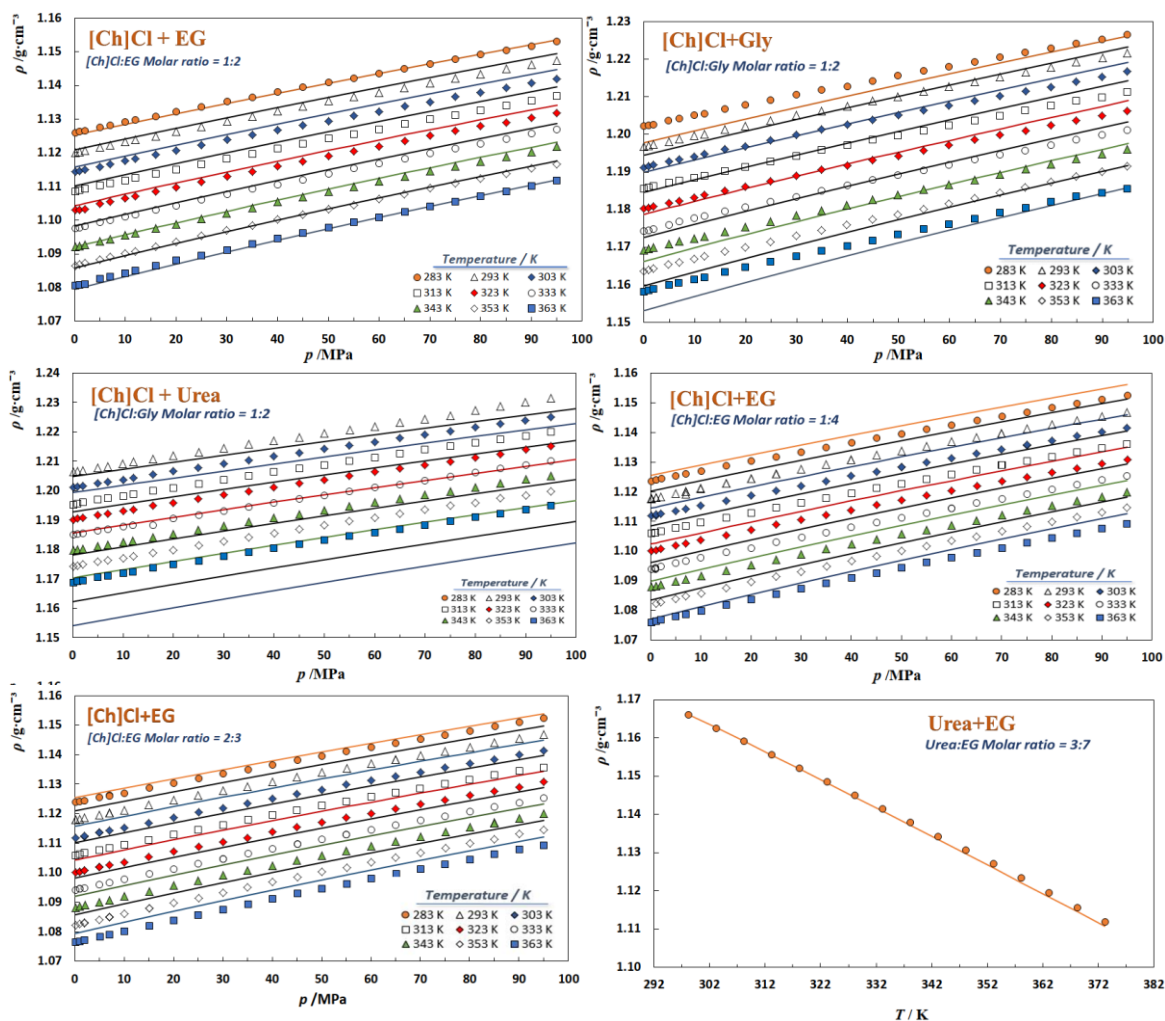


Figure 1.3 Density as a function of temperature and pressure for the three DES studied plus the mixture urea with ethylene glycol. The solid lines represent the soft-SAFT results.

5.3 Viscosity modeling results

Having the molecular parameters optimized, it is time to optimize the viscosity parameters that come from free volume theory formulated by Allal et al.^[82]. There is no information in literature about the values for the pure compounds parameters. Thus, to determine the parameters viscosity data of the pure compounds is required. As for the case of density an optimization Matlab routine was developed aiming at determining the compounds' parameters and using the compounds' molecular parameters optimized before.

Ethylene glycol and glycerol were modeled using viscosity data reported by Sagdeev et al.^[112], for EG (in the 293.15 K and 464.40 K temperature range and for pressures up to 245.16

MPa), and Cook et al.^[113], for Glycerol (in the 313.15 K and 473.15 K temperature range and at atmospheric pressure), as depicted in **Figure 1.4**. The first substance which viscosity parameters were optimized was for ethylene glycol the values of parameters obtained are indicated in **Table 1.1**. Since EG and Gly are not much different (with glycerol having an extra OH and CH₂ groups), to optimize the viscosity parameters of glycerol the values of the EG viscosity parameters were used as an initial guess with the Matlab™ routine converging to the values reported in **Table 1.1**. The different attempts made to the optimization these compounds are reported in **Figure B.2** and B.3 in Appendix B.

To optimize the viscosity parameters for [Ch]Cl, viscosity data of [Ch]Cl + EG and [Ch]Cl + Gly mixtures were used. As depicted in **Figure B.5**, in appendix B, soft-SAFT was not able to properly describe the viscosity behavior of the mixtures. Thus, a temperature dependent parameter (B) was required to represent [Ch]Cl. Furthermore, aiming to keep the physical meaning of the optimized parameters, and not having literature values for the viscosity parameters of salts similar to [Ch]Cl, those of EG and Gly were used as reference (aiming at obtaining values in the same order of magnitude) and as initial guesses. The attempts made for the optimization of [Ch]Cl are reported in **Table B.4**, in Appendix B, and the optimized parameters reported in **Table 1.1**. For urea, viscosity data of [Ch]Cl + Urea, at atmospheric pressure, was used keeping as criteria an α around those obtained for EG and Gly. The attempts for the urea optimization are reported in **Table B.1**, in Appendix B, and the optimized parameters reported in **Figure B.6**. With the molecular and viscosity parameters obtained for urea, it is possible to describe urea's properties and phase equilibria at all the systems evaluated.

The observation of the **Figure 1.4** and **Figure 1.5** allows to conclude that generally the atmospheric pressure is well described for all the compounds.

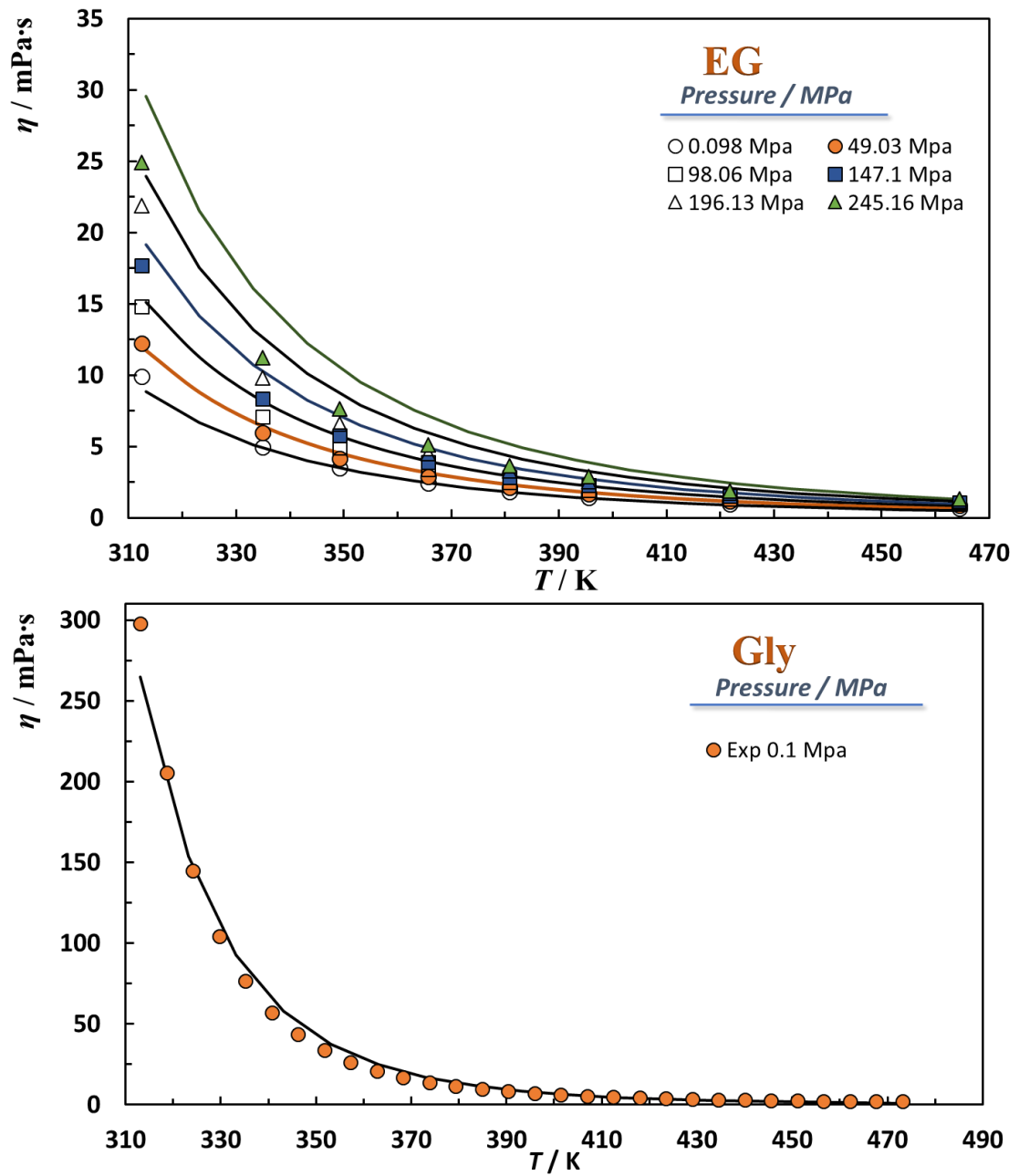


Figure 1.4. Viscosity of ethylene glycol and glycerol in function of the temperature and pressure. The solid lines represent the soft-SAFT EoS description.

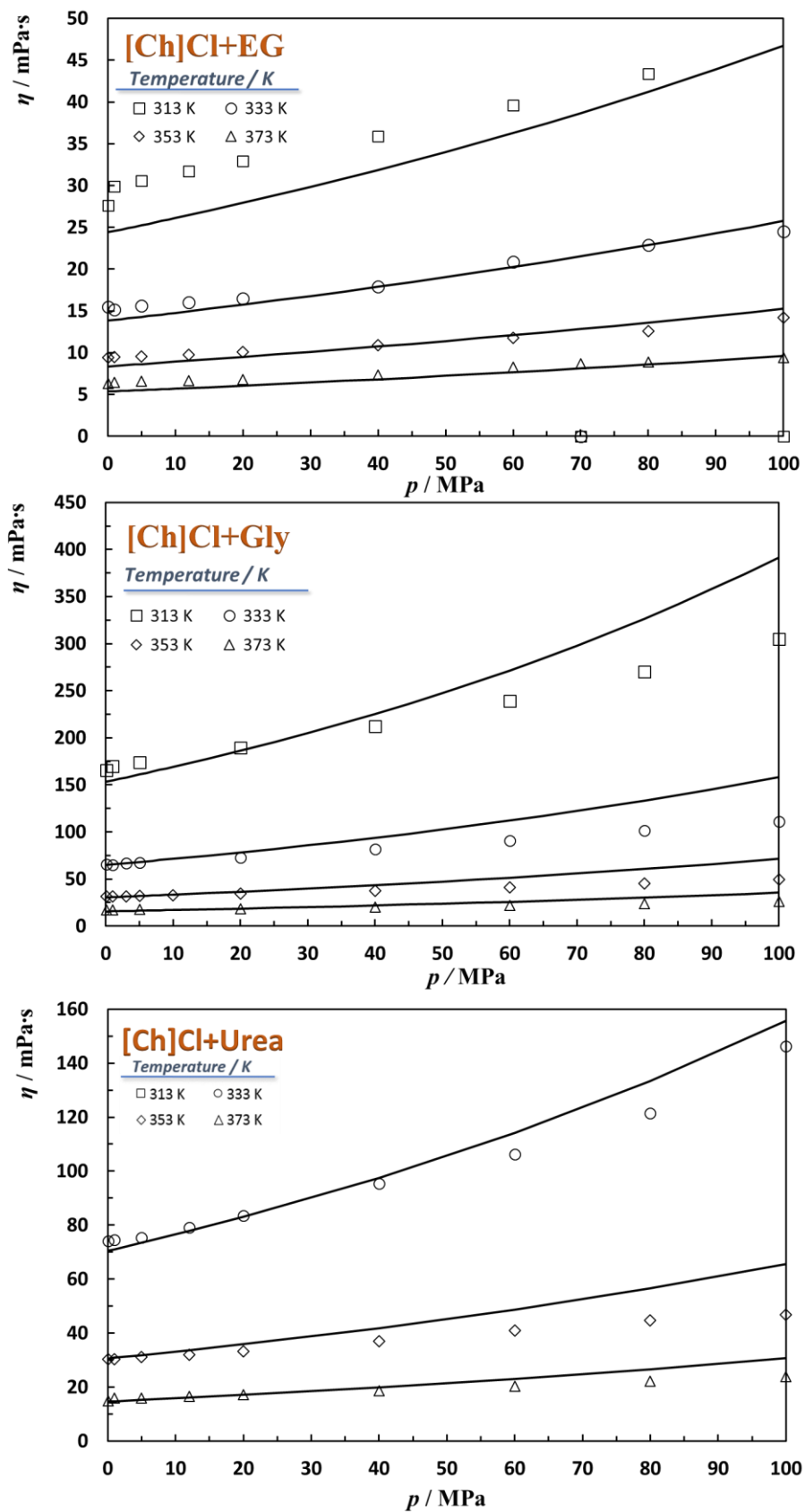


Figure 1.5. Viscosity as function of temperature and pressure for the three DES evaluated. The solid lines represent the soft-SAFT EoS description.

Table 1.1. soft-SAFT molecular and viscosity parameters gathered from literature^{[66],[114]} and those optimized in this work.

Parameter	Substance			
	[Ch]Cl	EG	Glycerol	Urea
m	4.359	1.751 ^[66]	2.344	2.896
σ (Å)	3.598	3.668 ^[66]	3.666	2.988
ε/k_B (K)	417.62	326.05 ^[66]	392.03	395.22
ε^{HB}/k_B ⁽¹⁾ (K)	3384	4384 ^[66]	4945	1695 ^[114]
ε^{HB}/k_B ⁽²⁾ (K)	3450	-	-	434.4
kHB ⁽¹⁾ (Å ³)	2100	4195 ^[66]	2250	2000 ^[114]
kHB ⁽²⁾ (Å ³)	2250	-	-	2000
α (J·m ³ /mol·kg)	202.31	214.00	220.00	189.30
B	$9.74 \cdot 10^{-03}$	$5.45 \cdot 10^{-03}$	$8.92 \cdot 10^{-03}$	$1.20 \cdot 10^{-02}$
B_1 (K ⁻¹)	$2.25 \cdot 10^{-05}$	-	-	-
L_v (Å)	$2.27 \cdot 10^{-02}$	$7.25 \cdot 10^{-02}$	$1.28 \cdot 10^{-02}$	$1.00 \cdot 10^{-02}$

- (1) stands for the cross-association energy and volume for the ions pair for [Ch]Cl, hydroxyl group for EG and Gly, and for the amine group for urea. ⁽²⁾ stands for the cross-association energy and volume for the hydroxyl group for [Ch]Cl, and for the ketone group for urea

Table 1.2. soft-SAFT binary interaction parameters used for each system.

Parameter	Mixture			
	[Ch]Cl + EG	[Ch]Cl + Gly	[Ch]Cl + Urea	Urea + EG
η	1.0000	1.0000	1.0000	1.1466
ζ	1.0624	1.0000	0.9840	1.0000

6. Conclusion

Aiming at reducing the environmental impact imposed by the use of conventional organic solvents while further answering the call of environment legislations and governmental expectations, the investigation of DES as solvents with high potential for a large number of applications and able to replace common organic solvents has motivated this work. Although DES have been proposed as solvents with a great potential, with a large number of constantly increasing publications, their use on real processes or simple scale-ups have been hampered by the insufficient thermophysical characterization and consequent accurate description by thermodynamic models, or correlations. The first objective of this is to increment the knowledge on the thermophysical properties, namely at high pressure (0.07 MPa – 100 MPa) density, viscosity and boiling temperatures, of the three most common eutectic mixtures of [Ch]Cl + EG, urea and glycerol at temperature ranging from (283.15 K and 373.15 K). Different techniques, namely a high pressure densimeter from Anton Paar (DMA-HPM), a high-pressure falling body viscosimeter, a vibrating wire viscosimeter and an atmospheric pressure SVM3000 densimeter/viscometer from Anton Paar were calibrated, evaluated for adequacy to perform the proposed measurements and used to obtain the reported experimental data.

Furthermore, the evaluated properties allowed to infer about the accuracy and capability of soft-SAFT EoS to model these neoteric solvents. New molecular models and parameters for the DES constituents were proposed and used to accurately describe the experimental data.

The models developed in this work can be implemented in commercial process simulator and foster the use of DES to industrial applications. Following the work of Crespo et al.^[108], where the author modeled the [Ch]Cl as LJ chains with five associating sites, “A” and “B” mimicking the hydroxyl group, a pair “C” and “D” sites mimicking the cation and anion interactions and an additional “C” site that represents the hydrogen bond acceptor character of the methyl groups this work proposes to model urea as LJ chains with three associating sites, “G” and “H” mimicking the hydrogen atoms of the hydroxyl group and a site “I” the lone pair of electrons in nitrogen, respectively. The corresponding molecular parameters and a state-independent binary interaction parameter were then regressed from experimental high-pressure liquid densities (measured in this work) and vapor-liquid equilibria of the Urea + EG.

7. Final Remarks and Future Work

The work presented in this thesis stands as a small contribution to that really necessary to foster the field. Thus, additional experimental data both to the mixtures evaluated here as for others stands vital and highly relevant. Furthermore, characterizing the DES on their entire composition range, not only on their eutectic composition, is also highly important if one aims at characterizing these neoteric solvents. On top of this characterization, further develop soft-SAFT EoS to be able to describe these complex systems aiming at its implementation in process simulation software is also extremely relevant while highly challenging and rewarding.

8. References

- (1) Smith, E. L.; Abbott, A. P.; Ryder, K. S. Deep Eutectic Solvents (DESs) and Their Applications. *Chem. Rev.* **2014**, *114*, 11060–11082.
- (2) Jafari, M. J.; Karimi, A.; Rezazadeh Azari, M. The Challenges of Controlling Organic Solvents in a Paint Factory Due to Solvent Impurity. *Ind. Health* **2009**, *47* (3), 326–332.
- (3) Park, H.; Park, H. D.; Jang, J. K. Exposure Characteristics of Construction Painters to Organic Solvents. *Saf. Health Work* **2016**, *7* (1), 63–71.
- (4) de Meijer, M. *Interactions Between Wood and Coatings With Low Organic Solvent Content*; Landbouwwun, Ed.; by Mari de Meijer: Wageningen, 1999.
- (5) Metha, S.; Besore, T. *Alternatives to Organic Solvent in Metal-Cleaning Operations*; Illinois Hazardous Waste Research & Information Center Dr. David L. Thomas, Savoy, 1989.
- (6) Worksafe Australia. *Industrial Organic Solvents*; National Occupational Health and Safety Commission, Ed.; Australian Government Publishing Service Canberra: Canberra, 1990.
- (7) Brostow, W. O n Swelling of Natural Rubber in Organic Solvents. *Macromolecules* **1965**, *1833* (4), 742–747.
- (8) Wibawa, G.; Takahashi, M.; Sato, Y.; Takishima, S.; Masuoka, H. Solubility of Seven Nonpolar Organic Solvents in Four Polymers Using the Piezoelectric-Quartz Sorption Method. *J. Chem. Eng. Data* **2002**, *47* (3), 518–524.
- (9) Elgal, G. M.; Ruppenicker, G. F.; Knoepfler, N. B.; Regional, S.; Orleans, N. Sizing and Desizing Textiles with Degraded Starch and Ultrasonic Techniques to Conserve Energy. *Energy Conserv. Text. Polym. Process.* **1979**, *107*, 127–143.
- (10) Walden, P.; Molekulargr, U. XJeber Die JVIolekulargrosse Und Elektriselie Leitfähigkeit Einiger Geschmolzenen Salze. *Bull. l'Académie Impériale des Sci. St.-pétersbg.* **1914**, *8* (6), 405–422.
- (11) Capela, E. V; Coutinho, J. A. P.; Freire, M. G. Application of Ionic Liquids in Separation and Fractionation Processes BT - Encyclopedia of Sustainability Science and Technology; Meyers, R. A., Ed.; Springer New York: New York, NY, 2018; pp 1–29.
- (12) Hallett, J. P.; Welton, T. Room-Temperature Ionic Liquids: Solvents for Synthesis and Catalysis. 2. *Chem. Rev.* **2011**, *111* (5), 3508–3576.
- (13) Rogers, R. D.; Seddon, K. R. Ionic Liquids — Solvents of the Future ? Alabama 2003, pp 792–793.

- (14) Pretti, C.; Chiappe, C.; Pieraccini, D.; Gregori, M.; Abramo, F.; Monni, G.; Intorre, L. Acute Toxicity of Ionic Liquids to the Zebrafish (*Danio Rerio*). *Green Chem.* **2006**, *8* (3), 238–240.
- (15) Marsh, K.; Boxall, J. A.; Lichtenthaler, R. Room Temperature Ionic Liquids and Their Mixtures—A Review. *Fluid Phase Equilib.* **2004**, *219*, 93–98.
- (16) Wang, H.; Lu, Q.; Ye, C.; Liu, W.; Cui, Z. Friction and Wear Behaviors of Ionic Liquid of Alkylimidazolium Hexafluorophosphates as Lubricants for Steel/Steel Contact. *Wear* **2004**, *256* (1–2), 44–48.
- (17) Bösmann, A.; Datsevich, L.; Jess, A.; Lauter, A.; Schmitz, C.; Wasserscheid, P. Deep Desulfurization of Diesel Fuel by Extraction with Ionic Liquids. *Chem. Commun.* **2001**, *0* (23), 2494–2495.
- (18) Wu, B.; Reddy, R. G.; Rogers, R. D. Novel Ionic Liquid Thermal Storage for Solar Thermal Electric Power Systems. In *Solar Energy: The Power to Choose*; Washington, DC, 2001.
- (19) Yanes, E. G.; Gratz, S. R.; Baldwin, M. J.; Robison, S. E.; Stalcup, A. M. Capillary Electrophoretic Application of 1-Alkyl-3-Methylimidazolium-Based Ionic Liquids. *Anal. Chem.* **2001**, *73* (16), 3838–3844.
- (20) Zell, C. A.; Freyland, W. In Situ STM and STS Study of Co and Co–Al Alloy Electrodeposition from an Ionic Liquid. *Langmuir* **2003**, *19* (18), 7445–7450.
- (21) Scovazzo, P.; Kieft, J.; Finan, D.; Koval, C.; Dubois, D.; Noble, R. Gas Separations Using Non-Hexafluorophosphate [PF₆]⁻ Anion Supported Ionic Liquid Membranes. *J. Memb. Sci.* **2004**, *238* (1–2), 57–63.
- (22) Jork, C.; Seiler, M.; Beste, Y.-A.; Arlt, W. Influence of Ionic Liquids on the Phase Behavior of Aqueous Azeotropic Systems. *J. Chem. Eng. Data* **2004**, *49* (4), 852–857.
- (23) Marsousi, S.; Karimi-Sabet, J.; Moosavian, M. A.; Amini, Y. Liquid-Liquid Extraction of Calcium Using Ionic Liquids in Spiral Microfluidics. *Chem. Eng. J.* **2019**, *356*, 492–505.
- (24) Karpińska, M.; Domańska, U. Liquid-Liquid Extraction of Styrene from Ethylbenzene Using Ionic Liquids. *J. Chem. Thermodyn.* **2018**, *124*, 153–159.
- (25) Fan, Y.; Xu, C.; Li, J.; Zhang, L.; Yang, L.; Zhou, Z.; Zhu, Y.; Zhao, D. Ionic Liquid-Based Microwave-Assisted Extraction of Verbascoside from *Rehmannia* Root. *Ind. Crops Prod.* **2018**, *124*, 59–65.
- (26) Sun, Y.; Zhang, S.; Zhang, X.; Zheng, Y.; Xiu, Z. Ionic Liquid-Based Sugaring-out and Salting-out Extraction of Succinic Acid. *Sep. Purif. Technol.* **2018**, *204* (2), 133–140.
- (27) Matsumiya, M.; Sumi, M.; Uchino, Y.; Yanagi, I. Recovery of Indium Based on the Combined Methods of Ionic Liquid Extraction and Electrodeposition. *Sep. Purif. Technol.* **2018**, *201*, 25–29.

- (28) Branco, L. C.; Crespo, J. G.; Afonso, C. a M. Studies on the Selective Transport of Organic Compounds by Using Ionic Liquids as Novel Supported Liquid Membranes. *Chem. - A Eur. J.* **2002**, *8* (17), 3865–3871.
- (29) Khandelwal, S.; Tailor, Y. K.; Kumar, M. Deep Eutectic Solvents (DESs) as Eco-Friendly and Sustainable Solvent/Catalyst Systems in Organic Transformations. *J. Mol. Liq.* **2016**, *215*, 345–386.
- (30) Vekariya, R. L. A Review of Ionic Liquids: Applications towards Catalytic Organic Transformations. *J. Mol. Liq.* **2017**, *227*, 44–60.
- (31) Dong, K.; Liu, X.; Dong, H.; Zhang, X.; Zhang, S. Multiscale Studies on Ionic Liquids. *Chem. Rev.* **2017**, *117* (10), 6636–6695.
- (32) Ghandi, K. A Review of Ionic Liquids , Their Limits and Applications. *Green Sustain. Chem.* **2014**, *4*, 44–53.
- (33) Ramesh, S.; Shanti, R.; Morris, E. Characterization of Conducting Cellulose Acetate Based Polymer Electrolytes Doped with “ Green ” Ionic Mixture. *Carbohydr. Polym.* **2013**, *91* (1), 14–21.
- (34) Martins, A. R.; Bu, M.; Ferreira, O.; Crespo, E. A.; Silva, L. P.; Pinho, P.; Sadowski, G.; Held, C. The Role of Polyfunctionality in the Formation of [Ch] Cl-Carboxylic Acid-Based Deep Eutectic Solvents. *Ind. Eng. Chem. Res.* **2018**, *57* (32), 11195–11209.
- (35) Abbott, A. P.; Capper, G.; Davies, D. L.; Rasheed, R. K.; Tambyrajah, V. Novel Solvent Properties of Choline Chloride / Urea Mixtures †. *R. Soc. Chem.* **2003**, No. October 2002, 70–71.
- (36) Abbott, A. P.; Harris, R. C.; Ryder, K. S.; D’Agostino, C.; Gladden, L. F.; Mantle, M. D. Glycerol Eutectics as Sustainable Solvent Systems. *Green Chem.* **2011**, *13* (1), 82–90.
- (37) Navarro, P.; Crespo, E. A.; Costa, J.; Llovel, F.; Garcia, J.; Rodríguez, F.; Carvalho, P. J.; Vega, L. F.; Coutinho, J. A. P. New Experimental Data and Modeling of Glymes : Towards the Development of a Predictive Model for Polyethers. *Ind. Eng. Chem. Res.* **2017**, *56*, 7830–7844.
- (38) Mjalli, F. S.; Naser, J.; Jibril, B.; Alizadeh, V.; Gano, Z. Tetrabutylammonium Chloride Based Ionic Liquid Analogues and Their Physical Properties. *J. Chem. Eng. Data* **2014**, *59* (7), 2242–2251.
- (39) Abbott, A. P.; Boothby, D.; Capper, G.; Davies, D. L.; Rasheed, R. K. Deep Eutectic Solvents Formed between Choline Chloride and Carboxylic Acids: Versatile Alternatives to Ionic Liquids. *J. Am. Chem. Soc.* **2004**, *126* (29), 9142–9147.
- (40) Francisco, M.; van den Bruinhorst, A.; Kroon, M. C. Low-Transition-Temperature Mixtures (LTTMs): A New Generation of Designer Solvents. *Angew. Chemie Int. Ed.* **2013**, *52* (11), 3074–3085.

- (41) Florindo, C.; Oliveira, F. S.; Rebelo, L. P. N.; Fernandes, A. M.; Marrucho, I. M. Insights into the Synthesis and Properties of Deep Eutectic Solvents Based on Cholinium Chloride and Carboxylic Acids. *ACS Sustain. Chem. Eng.* **2014**, *2* (10), 2416–2425.
- (42) Mukhopadhyay, S.; Mukherjee, S.; Hayyan, A.; Hayyan, M. Enhanced Removal of Lead from Contaminated Soil by Polyol-Based Deep Eutectic Solvents and Saponin. *J. Contam. Hydrol.* **2016**, *194*, 17–23.
- (43) Hayyan, A.; Mjalli, F. S.; Alnashef, I. M.; Al-wahaibi, Y. M.; Al-wahaibi, T.; Ali, M. Glucose-Based Deep Eutectic Solvents : Physical Properties. *J. Mol. Liq.* **2013**, *178*, 137–141.
- (44) Guo, W.; Hou, Y.; Ren, S.; Tian, S.; Wu, W. Formation of Deep Eutectic Solvents by Phenols and Choline Chloride and Their Physical Properties. *J. Chem. Eng. Data* **2013**, *58* (4), 866–872.
- (45) Sitze, M. S.; Schreiter, E. R.; Patterson, E. V.; Freeman, R. G. Ionic Liquids Based on FeCl₃ and FeCl₂. Raman Scattering and Ab Initio Calculations. *Inorg. Chem.* **2001**, *40* (10), 2298–2304.
- (46) Abbott, A. P.; Capper, G.; Davies, D. L.; Rasheed, R. K.; Tambyrajah, V. Novel Solvent Properties of Choline Chloride/Urea Mixtures. *Chem. Commun.* **2003**, 70–71.
- (47) Abbott, A. P.; Bell, T. J.; Handa, S.; Stoddart, B. Cationic Functionalisation of Cellulose Using a Choline Based Ionic Liquid Analogue. *Green Chem.* **2006**, *8* (9), 784–786.
- (48) Abbott, A. P.; Capper, G.; Davies, D. L.; McKenzie, K. J.; Obi, S. U. Solubility of Metal Oxides in Deep Eutectic Solvents Based on Choline Chloride. *J. Chem. Eng. Data* **2006**, *51* (4), 1280–1282.
- (49) Abbott, A. P.; Cullis, P. M.; Gibson, M. J.; Harris, R. C.; Raven, E. Extraction of Glycerol from Biodiesel into a Eutectic Based Ionic Liquid. *Green Chem.* **2007**, *9*, 868–872.
- (50) Abbott, A. P.; Barron, J. C.; Ryder, K. S.; Wilson, D. Eutectic-Based Ionic Liquids with Metal-Containing Anions and Cations. *Chem. - A Eur. J.* **2007**, *13* (22), 6495–6501.
- (51) Agostino, C. D.; Harris, R. C.; Abbott, A. P.; Gladden, F.; Mantle, M. D. Molecular Motion and Ion Diffusion in Choline Chloride Based Deep Eutectic Solvents Studied by ¹H Pulsed Field Gradient NMR Spectroscopy. *Phys. Chem. Chem. Phys.* **2011**, *13*, 21383–21391.
- (52) Jibril, B.; Mjalli, F.; Naser, J.; Gano, Z. New Tetrapropylammonium Bromide-Based Deep Eutectic Solvents: Synthesis and Characterizations. *J. Mol. Liq.* **2014**, *199*, 462–469.
- (53) Mjalli, F. S.; Jabbar, N. M. A. Acoustic Investigation of Choline Chloride Based Ionic

- Liquids Analogs. *Fluid Phase Equilib.* **2014**, *381*, 71–76.
- (54) Mjalli, F. S.; Vakili-Nezhaad, G.; Shahbaz, K.; Alnashef, I. M. Application of the Eötvös and Guggenheim Empirical Rules for Predicting the Density and Surface Tension of Ionic Liquids Analogues. *Thermochim. Acta* **2014**, *575*, 40–44.
- (55) Abbott, A. P.; Capper, G.; Gray, S. Design of Improved Deep Eutectic Solvents Using Hole Theory. *ChemicalPhysChem* **2006**, *7* (4), 803–806.
- (56) Bandr, I.; Alcalde, R.; Lafuente, C.; Atilhan, M.; Aparicio, S. On the Viscosity of Pyridinium Based Ionic Liquids: An Experimental and Computational Study. *J. Phys. Chem. B* **2011**, *115*, 12499–12513.
- (57) Bagh, F. S. G.; Shahbaz, K.; Mjalli, F. S.; AlNashef, I. M.; Hashim, M. A. Electrical Conductivity of Ammonium and Phosphonium Based Deep Eutectic Solvents: Measurements and Artificial Intelligence-Based Prediction. *Fluid Phase Equilib.* **2013**, *356*, 30–37.
- (58) Bahadori, L.; Chakrabarti, M. H.; Mjalli, F. S.; Alnashef, I. M.; Manan, N. S. A.; Hashim, M. A. Physicochemical Properties of Ammonium-Based Deep Eutectic Solvents and Their Electrochemical Evaluation Using Organometallic Reference Redox Systems. *Electrochim. Acta* **2013**, *113*, 205–211.
- (59) Yadav, A.; Pandey, S. Densities and Viscosities of (Choline Chloride + Urea) Deep Eutectic Solvent and Its Aqueous Mixtures in the Temperature Range 293.15 K to 363.15 K. *J. Chem. Eng. Data* **2014**, *59* (7), 2221–2229.
- (60) Yadav, A.; Trivedi, S.; Rai, R.; Pandey, S. Fluid Phase Equilibria Densities and Dynamic Viscosities of (Choline Chloride + Glycerol) Deep Eutectic Solvent and Its Aqueous Mixtures in the Temperature Range. *Fluid Phase Equilib.* **2014**, *367*, 135–142.
- (61) Yadav, A.; Rani, J.; Verma, M.; Naqvi, S.; Pandey, S. *Thermochimica Acta* Densities of Aqueous Mixtures of (Choline Chloride + Ethylene Glycol) and (Choline Chloride + Malonic Acid) Deep Eutectic Solvents In. *Thermochim. Acta* **2015**, *600*, 95–101.
- (62) Shahbaz, K.; Baroutian, S.; Mjalli, F. S.; Hashim, M. A.; Alnashef, I. M. Densities of Ammonium and Phosphonium Based Deep Eutectic Solvents: Prediction Using Artificial Intelligence and Group Contribution Techniques. *Thermochim. Acta* **2012**, *527*, 59–66.
- (63) Shahbaz, K.; Bagh, F. S. G.; Mjalli, F. S.; AlNashef, I. M.; Hashim, M. A. Prediction of Refractive Index and Density of Deep Eutectic Solvents Using Atomic Contributions. *Fluid Phase Equilib.* **2013**, *354*, 304–311.
- (64) Leron, R. B.; Li, M. *Thermochimica Acta* High-Pressure Volumetric Properties of Choline Chloride – Ethylene Glycol Based Deep Eutectic Solvent and Its Mixtures with Water. *Thermochim. Acta* **2012**, *546*, 54–60.
- (65) Ahrens, T. J. *Equation of State*; Springer New York: New York, NY, 2013; Vol. 1.

- (66) Crespo, E. A.; Costa, J.; Navarro, P.; Crespo, E. A. New Experimental Data and Modeling of Glymes: Toward the Development of a Predictive Model for Polyethers. *Ind. Eng. Chem. Res.* **2017**, *56* (27), 7830–7844.
- (67) Feng, Z.; Panuganti, S. R.; Chapman, W. G. Predicting Solubility and Swelling Ratio of Blowing Agents in Rubbery Polymers Using PC-SAFT Equation of State. *Chem. Eng. Sci.* **2018**, *183*, 306–328.
- (68) Chapman, W. G.; Jackson, G.; Gubbins, K. E. Phase Equilibria of Associating Fluids. *Mol. Phys.* **1988**, *65* (5), 1057–1079.
- (69) Chapman, W.; Gubbins, K.; Jackson, G.; Radosz, M. New Reference Equation of State for Associating Fluids. *Ind. Eng. Chem. Res.* **1990**, *29*, 1709–1721.
- (70) Wertheim, M. S. Fluids with Highly Directional Attractive Forces. III. Multiple Attraction Sites. *J. Stat. Phys.* **1986**, *42* (3–4), 459–476.
- (71) Marshall, B. D.; Bokis, C. P. A PC-SAFT Model for Hydrocarbons II: General Model Development. *Fluid Phase Equilib.* **2018**, 1–8.
- (72) Palma, A. M.; Oliveira, M. B.; Queimada, A. J.; Coutinho, J. A. P. Re-Evaluating the CPA EoS for Improving Critical Points and Derivative Properties Description. *Fluid Phase Equilib.* **2017**, *436*, 85–97.
- (73) Belkadi, A.; Hadj-Kali, M. K.; Gerbaud, V.; Joulia, X.; Llovel, F.; Vega, L. F. Modeling the Phase Equilibria of Nitriles by the Soft-SAFT Equation of State. *Comput. Aided Chem. Eng.* **2008**, *25*, 739–744.
- (74) Pereira, L. M. C.; Martins, V.; Kurnia, K. A.; Oliveira, M. B.; Dias, A. M. A.; Llovel, F.; Vega, L. F.; Carvalho, P. J.; Coutinho, J. A. P. High Pressure Solubility of CH₄, N₂O and N₂ in 1-Butyl-3-Methylimidazolium Dicyanamide: Solubilities, Selectivities and Soft-SAFT Modeling. *J. Supercrit. Fluids* **2016**, *110*, 56–64.
- (75) Pereira, L. M. C.; Oliveira, M. B.; Llovel, F.; Vega, L. F.; Coutinho, J. A. P. Assessing the N₂O/CO₂ high Pressure Separation Using Ionic Liquids with the Soft-SAFT EoS. *J. Supercrit. Fluids* **2014**, *92*, 231–241.
- (76) Oliveira, M. B.; Freitas, S. V.D.; Llovel, F.; Vega, L. F.; Coutinho, J. A. P. Development of Simple and Transferable Molecular Models for Biodiesel Production with the Soft-SAFT Equation of State. *Chem. Eng. Res. Des.* **2014**, *92* (12), 1898–1911.
- (77) Crespo, E.; Carvalho, P.; Coutinho, J.; Vega, L. Exploring Alternative Solvents for Gas Processing Using the Soft-SAFT EoS. In *RD PETRO 2018: Research and Development Petroleum Conference and Exhibition, Abu Dhabi, UAE, 9-10 May 2018*; Abu Dhabi, 2018; pp 156–160.
- (78) Crespo, E. A.; Amaral, M.; Dariva, C.; Carvalho, P. J.; Coutinho, J. A. P.; Vega, L. F. Soft-SAFT Equation of State as a Valuable Tool for the Design of New CO₂ Capture Technologies. *Abu Dhabi International Petroleum Exhibition & Conference*. Society of Petroleum Engineers: Abu Dhabi, UAE 2017, p 13.

- (79) Blas, F. J.; Vega, L. F. Thermodynamic Behaviour of Homonuclear and Heteronuclear Lennard-Jones Chains with Association Sites from Simulation and Theory. *Mol. Phys.* **1997**, *92* (1), 135–150.
- (80) Belkadi, A.; Hadj-Kali, M. K.; Llovel, F.; Gerbaud, V.; Vega, L. F. Soft-SAFT Modeling of Vapor-Liquid Equilibria of Nitriles and Their Mixtures. *Fluid Phase Equilib.* **2010**, *289* (2), 191–200.
- (81) Pàmies, J. C.; Vega, L. F. Vapor–Liquid Equilibria and Critical Behavior of Heavy *n* - Alkanes Using Transferable Parameters from the Soft-SAFT Equation of State. *Ind. Eng. Chem. Res.* **2001**, *40* (11), 2532–2543.
- (82) Allal, A.; Boned, C.; Baylaucq, A. Free-Volume Viscosity Model for Fluids in the Dense and Gaseous States. *Phys. Rev. E - Stat. Physics, Plasmas, Fluids, Relat. Interdiscip. Top.* **2001**, *64* (1).
- (83) Allal, A.; Moha-Ouchane, M.; Boned, C. A New Free Volume Model for Dynamic Viscosity and Density of Dense Fluids versus Pressure and Temperature. *Phys. Chem. Liq.* **2001**, *39* (1), 1–30.
- (84) Doolittle, A. K. Studies in Newtonian Flow. II. The Dependence of the Viscosity of Liquids on Free-Space. *J. Appl. Phys.* **1951**, *22* (12), 1471–1475.
- (85) Cohen, M. H.; Turnbull, D. Molecular Transport in Liquids and Glasses. *J. Chem. Phys.* **1959**, *31*, 1164–1169.
- (86) Llovel, F.; Marcos, R. M.; Vega, L. F. Free-Volume Theory Coupled with Soft-SAFT for Viscosity Calculations: Comparison with Molecular Simulation and Experimental Data. *J. Phys. Chem. B* **2013**, *117* (27), 8159–8171.
- (87) Llovel, F.; Marcos, R. M.; Vega, L. F. Transport Properties of Mixtures by the Soft-SAFT + Free-Volume Theory: Application to Mixtures of *n* -Alkanes and Hydrofluorocarbons. *J. Phys. Chem. B* **2013**, *117* (17), 5195–5205.
- (88) Polishuk, I.; Yitzhak, A. Modeling Viscosities of Pure Compounds and Their Binary Mixtures Using the Modified Yarranton-Satyro Correlation and Free Volume Theory Coupled with SAFT+Cubic EoS. *Ind. Eng. Chem. Res.* **2014**, *53* (2), 959–971.
- (89) Baylaucq, A.; Boned, C.; Canet, X.; Zéberg-Mikkelsen, C. K.; Quiñones-Cisneros, S. E.; Zhou, H. Dynamic Viscosity Modeling of Methane + N-Decane and Methane + Toluene Mixtures : Comparative Study of Some Representative Models. *Pet. Sci. Technol.* **2005**, *23* (2), 143–157.
- (90) Pedrosa, N.; Pàmies, J. C.; Coutinho, J. A. P.; Marrucho, I. M.; Vega, L. F. Phase Equilibria of Ethylene Glycol Oligomers and Their Mixtures. *Ind. Eng. Chem. Res.* **2005**, *44* (17), 7027–7037.
- (91) Concepción, E. I.; Gómez-Hernández, Á.; Martín, M. C.; Segovia, J. J. Density and Viscosity Measurements of Aqueous Amines at High Pressures: DEA-Water, DMAE-Water and TEA-Water Mixtures. *J. Chem. Thermodyn.* **2017**, *112*, 227–239.

- (92) Zambrano, J.; Martín, M. C.; Moreau, A.; Concepción, E. I.; Segovia, J. J. Viscosities of Binary Mixtures Containing 2-Butanol + hydrocarbons (2,2,4-Trimethylpentane or 1,2,4-Trimethylbenzene) at High Pressures for the Implementation of Second Generation Biofuels. *J. Chem. Thermodyn.* **2018**, *125*, 180–185.
- (93) Gaciño, F. M.; Comuñas, M. J. P.; Regueira, T.; Segovia, J. J.; Fernández, J. On the Viscosity of Two 1-Butyl-1-Methylpyrrolidinium Ionic Liquids: Effect of the Temperature and Pressure. *J. Chem. Thermodyn.* **2015**, *87*, 43–51.
- (94) Stuckenholtz, M.; Crespo, E. A.; Vega, L. F.; Carvalho, P. J.; Coutinho, J. A. P.; Schröer, W.; Kiefer, J.; Rathke, B. Vapor Liquid Equilibria of Binary Mixtures of 1-Butyl-3-Methylimidazolium Triflate (C4mimTfO) and Molecular Solvents: N-Alkyl Alcohols and Water. *J. Phys. Chem. B* **2018**, *122* (22), 6017–6032.
- (95) Leron, R. B.; Li, M. H. High-Pressure Density Measurements for Choline Chloride: Urea Deep Eutectic Solvent and Its Aqueous Mixtures at T = (298.15 to 323.15) K and up to 50 MPa. *J. Chem. Thermodyn.* **2012**, *54*, 293–301.
- (96) Leron, R. B.; Wong, D. S. H.; Li, M. H. Densities of a Deep Eutectic Solvent Based on Choline Chloride and Glycerol and Its Aqueous Mixtures at Elevated Pressures. *Fluid Phase Equilib.* **2012**, *335*, 32–38.
- (97) Leron, R. B.; Li, M.-H. Molar Heat Capacities of Choline Chloride-Based Deep Eutectic Solvents and Their Binary Mixtures with Water. *Thermochim. Acta* **2012**, *530*, 52–57.
- (98) Siongco, K. R.; Leron, R. B.; Li, M. H. Densities, Refractive Indices, and Viscosities of N,N-Diethylethanol Ammonium Chloride-Glycerol or -Ethylene Glycol Deep Eutectic Solvents and Their Aqueous Solutions. *J. Chem. Thermodyn.* **2013**, *65*, 65–72.
- (99) Silva, L. P.; Fernandez, L.; Conceição, J. H. F.; Martins, M. A. R.; Sosa, A.; Ortega, J.; Pinho, S. P.; Coutinho, J. A. P. Design and Characterization of Sugar-Based Deep Eutectic Solvents Using Conductor-like Screening Model for Real Solvents. *ACS Sustain. Chem. Eng.* **2018**, *6* (8), 10724–10734.
- (100) D'Agostino, C.; Harris, R. C.; Abbott, A. P.; Gladden, L. F.; Mantle, M. D. Molecular Motion and Ion Diffusion in Choline Chloride Based Deep Eutectic Solvents Studied by 1H Pulsed Field Gradient NMR Spectroscopy. *Phys. Chem. Chem. Phys.* **2011**, *13* (48), 21383–21391.
- (101) Falkovich, G. *Fluid Mechanics A Short Course for Physicists*; Cambridge University press: Cambridge, 2011.
- (102) Schmelzer, J. W. P.; Zanutto, E. D.; Fokin, V. M. Pressure Dependence of Viscosity. *J. Chem. Phys.* **2005**, *122* (7), 074511.
- (103) Crespo et Al., To Be Submitted.
- (104) Azevedo, F. G. D. E.; Oliveira, W. A. D. E. Ebulliometric Behaviour Solutions of Urea of Aqueous. *J. Chem. Thermodyn.* **1984**, *16*, 683–686.

- (105) Perman, E. P.; Lovett, T. Vapour Pressure and Heat of Dilution of Aqueous Solutions. *Trans. Faraday Soc.* **1926**, *XXII*, 19.
- (106) Hou, C.; Wang, G.; Zhang, B. Bubble Point Pressure of the Solutions of H₂SiF₆ + H₂O and H₂SiF₆ + CO(NH₂)₂ + H₂O from 323 K to 353 K. *J. Chem. Eng. Data* **2006**, *2* (1), 864–866.
- (107) Zubeir, L. F.; Held, C.; Sadowski, G.; Kroon, M. C. PC-SAFT Modeling of CO₂ Solubilities in Deep Eutectic Solvents. *J. Phys. Chem. B* **2016**, *120* (9), 2300–2310.
- (108) Ashworth, C. R.; Matthews, R. P.; Welton, T.; Hunt, P. A. Doubly Ionic Hydrogen Bond Interactions within the Choline Chloride–urea Deep Eutectic Solvent. *Phys. Chem. Chem. Phys.* **2016**, *18* (27), 18145–18160.
- (109) Lloret, J. O.; Vega, L. F.; Llorell, F. Fluid Phase Equilibria Accurate Description of Thermophysical Properties of Tetraalkylammonium Chloride Deep Eutectic Solvents with the Soft- SAFT Equation of State. *Fluid Phase Equilib.* **2017**, *448*, 81–93.
- (110) Held, C.; Neuhaus, T.; Sadowski, G. Compatible Solutes: Thermodynamic Properties and Biological Impact of Ectoines and Prolines. *Biophys. Chem.* **2010**, *152* (1–3), 28–39.
- (111) Pereira, L. M. C.; Llorell, F.; Vega, L. F. Thermodynamic Characterisation of Aqueous Alkanolamine and Amine Solutions for Acid Gas Processing by Transferable Molecular Models. *Appl. Energy* **2018**, *222*, 687–703.
- (112) Sagdeev, D. I.; Fomina, M. G.; Mukhamedzyanov, G. K.; Abdulagatov, I. M. Experimental Study of the Density and Viscosity of Polyethylene Glycols and Their Mixtures at Temperatures from 293 K to 473 K and at Atmospheric Pressure. *J. Chem. Thermodyn.* **2011**, *43* (12), 1824–1843.
- (113) Cook, R. L.; King, H. E.; Herbst, C. A.; Herschbach, D. R.; Cook, R. L.; King, H. E.; Herbst, J. C. A.; Herschbach, D. R. Pressure and Temperature Dependent Viscosity of Two Glass Forming Liquids : Glycerol and Dibutyl Phthalate. *J. Chem. Phys.* **1994**, *100* (7), 5178–5189.
- (114) Pereira, L. M. C.; Llorell, F.; Vega, L. F. Thermodynamic Characterisation of Aqueous Alkanolamine and Amine Solutions for Acid Gas Processing by Transferable Molecular Models. *Appl. Energy* **2018**, *222*, 687–703.

Appendix A – Experimental Results

Table A1. Density as function of pressure and temperature for the [Ch]Cl + EG eutectic mixture.

$\rho / \text{g}\cdot\text{cm}^{-3}$									
p / MPa	T / K								
	283.15	293.15	303.15	313.15	323.15	333.15	343.15	353.15	363.15
0.1	1.1260	1.1200	1.1143	1.1086	1.1031	1.0975	1.0921	1.0865	1.0806
1	1.1263	1.1203	1.1147	1.1090	1.1030	1.0979	1.0924	1.0868	1.0808
2	1.1266	1.1206	1.1150	1.1093	1.1033	1.0983	1.0928	1.0872	1.0810
5	1.1276	1.1217	1.1159	1.1103	1.1048	1.0994	1.0938	1.0884	1.0826
7	1.1282	1.1222	1.1166	1.1109	1.1055	1.1000	1.0945	1.0891	1.0833
10	1.1291	1.1232	1.1176	1.1119	1.1064	1.1011	1.0955	1.0901	1.0843
12	1.1298	1.1238	1.1182	1.1125	1.1071	1.1017	1.0963	1.0907	1.0851
16	1.1309	1.1250	1.1194	1.1137	1.1085	1.1030	1.0975	1.0922	1.0865
20	1.1322	1.1263	1.1208	1.1151	1.1097	1.1043	1.0988	1.0936	1.0880
25	1.1337	1.1278	1.1224	1.1167	1.1114	1.1061	1.1005	1.0953	1.0895
30	1.1352	1.1294	1.1238	1.1183	1.1129	1.1077	1.1021	1.0970	1.0912
35	1.1365	1.1308	1.1252	1.1197	1.1145	1.1093	1.1037	1.0985	1.0930
40	1.1381	1.1324	1.1268	1.1212	1.1160	1.1105	1.1054	1.1002	1.0946
45	1.1395	1.1339	1.1283	1.1227	1.1174	1.1121	1.1069	1.1016	1.0962
50	1.1408	1.1354	1.1294	1.1242	1.1190	1.1137	1.1085	1.1032	1.0978
55	1.1421	1.1368	1.1309	1.1256	1.1205	1.1153	1.1100	1.1046	1.0995
60	1.1436	1.1379	1.1323	1.1270	1.1219	1.1168	1.1116	1.1063	1.1009
65	1.1450	1.1394	1.1338	1.1285	1.1235	1.1183	1.1130	1.1078	1.1024
70	1.1465	1.1408	1.1351	1.1299	1.1250	1.1198	1.1146	1.1095	1.1041
75	1.1479	1.1421	1.1366	1.1312	1.1265	1.1212	1.1160	1.1110	1.1056
80	1.1492	1.1434	1.1379	1.1326	1.1279	1.1227	1.1174	1.1124	1.1070
85	1.1504	1.1449	1.1392	1.1341	1.1289	1.1242	1.1188	1.1137	1.1086
90	1.1517	1.1462	1.1407	1.1355	1.1305	1.1257	1.1203	1.1154	1.1102
95	1.1530	1.1475	1.1419	1.1369	1.1318	1.1270	1.1218	1.1167	1.1117

Standard uncertainty in the temperature, $u(T)$, is 0.01 K; Standard uncertainty in the pressure, $u(p)$, is 0.01 MPa; Combined Standard uncertainty in the density $u_r(\rho)$, is 0.0001 $\text{g}\cdot\text{cm}^{-3}$.

Table A2. Density as function of pressure and temperature for the [Ch]Cl + Gly eutectic mixture.

$\rho / \text{g}\cdot\text{cm}^{-3}$									
p / MPa	T / K								
	283	293	303	313	323	333	343	353	363
0.1	1.2022	1.1968	1.1912	1.1856	1.1803	1.1744	1.1693	1.1637	1.1581
1	1.2025	1.1970	1.1915	1.1859	1.1806	1.1746	1.1696	1.1640	1.1585
2	1.2026	1.1973	1.1918	1.1863	1.1808	1.1748	1.1699	1.1644	1.1589
5	1.2037	1.1982	1.1928	1.1872	1.1818	1.1759	1.1709	1.1654	1.1599
7	1.2042	1.1988	1.1933	1.1878	1.1824	1.1769	1.1715	1.1660	1.1606
10	1.2051	1.1997	1.1941	1.1885	1.1832	1.1778	1.1724	1.1670	1.1615
12	1.2056	1.2001	1.1948	1.1889	1.1839	1.1783	1.1729	1.1676	1.1621
16	1.2068	1.2013	1.1960	1.1902	1.1850	1.1796	1.1742	1.1689	1.1634
20	1.2078	1.2023	1.1969	1.1914	1.1862	1.1807	1.1753	1.1700	1.1646
25	1.2092	1.2036	1.1984	1.1928	1.1876	1.1822	1.1769	1.1715	1.1661
30	1.2106	1.2052	1.1999	1.1943	1.1890	1.1835	1.1784	1.1730	1.1677
35	1.2119	1.2063	1.2013	1.1959	1.1906	1.1851	1.1797	1.1746	1.1691
40	1.2128	1.2076	1.2025	1.1973	1.1917	1.1866	1.1812	1.1761	1.1703
45	1.2143	1.2089	1.2038	1.1986	1.1932	1.1879	1.1826	1.1774	1.1718
50	1.2156	1.2101	1.2051	1.1997	1.1943	1.1892	1.1839	1.1786	1.1734
55	1.2169	1.2115	1.2064	1.2010	1.1958	1.1905	1.1854	1.1802	1.1749
60	1.2181	1.2128	1.2076	1.2024	1.1972	1.1919	1.1866	1.1816	1.1761
65	1.2192	1.2140	1.2089	1.2038	1.1987	1.1934	1.1879	1.1831	1.1777
70	1.2206	1.2153	1.2103	1.2050	1.1999	1.1947	1.1894	1.1845	1.1792
75	1.2219	1.2165	1.2115	1.2064	1.2010	1.1958	1.1908	1.1859	1.1806
80	1.2229	1.2178	1.2127	1.2077	1.2025	1.1973	1.1921	1.1874	1.1822
85	1.2241	1.2192	1.2141	1.2089	1.2038	1.1986	1.1936	1.1888	1.1835
90	1.2253	1.2204	1.2153	1.2099	1.2049	1.1999	1.1948	1.1901	1.1845
95	1.2266	1.2216	1.2167	1.2114	1.2063	1.2011	1.1961	1.1915	1.1856

Standard uncertainty in the temperature, $u(T)$, is 0.01 K; Standard uncertainty in the pressure, $u(p)$, is 0.01 MPa; Combined Standard uncertainty in the density $u_r(\rho)$, is $0.0001 \text{ g}\cdot\text{cm}^{-3}$.

Table A3. Density as function of pressure and temperature for the [Ch]Cl + Urea eutectic mixture.

$\rho / \text{g.cm}^{-3}$								
p / MPa	T / K							
	293	303	313	323	333	343	353	363
0.1	1.2014	1.1961	1.1903	1.1852	1.1799	1.1747	1.1693	1.1638
1	1.2017	1.1964	1.1906	1.1856	1.1802	1.1750	1.1695	1.1642
2	1.2020	1.1967	1.1911	1.1859	1.1805	1.1753	1.1699	1.1645
5	1.2028	1.1974	1.1919	1.1868	1.1814	1.1761	1.1708	1.1655
7	1.2034	1.1980	1.1924	1.1871	1.1820	1.1767	1.1714	1.1661
10	1.2042	1.1987	1.1933	1.1881	1.1827	1.1775	1.1721	1.1669
12	1.2048	1.1994	1.1938	1.1885	1.1833	1.1781	1.1726	1.1675
16	1.2059	1.2005	1.1949	1.1899	1.1833	1.1792	1.1739	1.1688
20	1.2068	1.2016	1.1960	1.1909	1.1856	1.1803	1.1748	1.1699
25	1.2081	1.2029	1.1972	1.1921	1.1868	1.1816	1.1763	1.1712
30	1.2095	1.2041	1.1987	1.1935	1.1882	1.1830	1.1777	1.1727
35	1.2108	1.2054	1.2001	1.1947	1.1896	1.1844	1.1791	1.1742
40	1.2120	1.2067	1.2013	1.1961	1.1909	1.1858	1.1805	1.1755
45	1.2132	1.2078	1.2025	1.1974	1.1923	1.1870	1.1819	1.1770
50	1.2146	1.2092	1.2038	1.1987	1.1934	1.1884	1.1832	1.1782
55	1.2157	1.2104	1.2051	1.2000	1.1948	1.1896	1.1846	1.1795
60	1.2168	1.2117	1.2063	1.2014	1.1961	1.1910	1.1858	1.1807
65	1.2181	1.2129	1.2076	1.2025	1.1972	1.1923	1.1871	1.1819
70	1.2193	1.2142	1.2089	1.2038	1.1985	1.1936	1.1886	1.1833
75	1.2206	1.2153	1.2101	1.2050	1.1999	1.1948	1.1898	1.1846
80	1.2223	1.2166	1.2112	1.2063	1.2012	1.1961	1.1910	1.1860
85	1.2238	1.2177	1.2125	1.2075	1.2026	1.1975	1.1924	1.1871
90	1.2252	1.2189	1.2137	1.2089	1.2038	1.1989	1.1934	1.1885
95	1.2265	1.2201	1.2149	1.2101	1.2052	1.2001	1.1948	1.1899

Standard uncertainty in the temperature, $u(T)$, is 0.01 K; Standard uncertainty in the pressure, $u(p)$, is 0.01 MPa; Combined Standard uncertainty in the density $u_r(\rho)$, is 0.0001 g.cm^{-3}

Table A4. Density as function of pressure and temperature for the [Ch]Cl + EG mixture with 2:3 molar ratio.

$\rho / \text{g.cm}^{-3}$									
p / MPa	T / K								
	283	293	303	313	323	333	343	353	363
0.1	1.1238	1.1179	1.1119	1.1059	1.1000	1.0941	1.0883	1.0823	1.0764
1	1.1241	1.1183	1.1122	1.1063	1.1004	1.0945	1.0886	1.0827	1.0766
2	1.1245	1.1186	1.1125	1.1067	1.1008	1.0948	1.0890	1.0830	1.0771
5	1.1255	1.1195	1.1137	1.1077	1.1018	1.0960	1.0900	1.0841	1.0783
7	1.1261	1.1202	1.1136	1.1084	1.1018	1.0967	1.0908	1.0849	1.0790
10	1.1261	1.1213	1.1143	1.1094	1.1025	1.0977	1.0920	1.0861	1.0801
12	1.1270	1.1229	1.1153	1.1112	1.1036	1.0995	1.0937	1.0879	1.0801
16	1.1288	1.1245	1.1169	1.1128	1.1054	1.1012	1.0957	1.0879	1.0819
20	1.1302	1.1262	1.1186	1.1145	1.1072	1.1031	1.0974	1.0897	1.0838
25	1.1319	1.1278	1.1204	1.1161	1.1087	1.1047	1.0991	1.0914	1.0857
30	1.1336	1.1292	1.1218	1.1180	1.1104	1.1047	1.1007	1.0932	1.0876
35	1.1351	1.1308	1.1235	1.1195	1.1119	1.1081	1.1024	1.0950	1.0893
40	1.1366	1.1324	1.1252	1.1211	1.1139	1.1097	1.1041	1.0968	1.0912
45	1.1381	1.1340	1.1267	1.1227	1.1154	1.1097	1.1059	1.0985	1.0929
50	1.1395	1.1353	1.1282	1.1242	1.1170	1.1130	1.1075	1.1002	1.0946
55	1.1410	1.1369	1.1298	1.1257	1.1186	1.1129	1.1090	1.1018	1.0963
60	1.1425	1.1383	1.1313	1.1272	1.1201	1.1145	1.1106	1.1035	1.0980
65	1.1439	1.1383	1.1327	1.1271	1.1216	1.1161	1.1124	1.1051	1.0995
70	1.1454	1.1397	1.1341	1.1286	1.1233	1.1177	1.1139	1.1067	1.1013
75	1.1467	1.1411	1.1357	1.1302	1.1247	1.1192	1.1155	1.1084	1.1029
80	1.1480	1.1426	1.1369	1.1315	1.1261	1.1207	1.1169	1.1100	1.1045
85	1.1496	1.1440	1.1385	1.1332	1.1277	1.1222	1.1169	1.1114	1.1062
90	1.1509	1.1455	1.1399	1.1344	1.1290	1.1238	1.1185	1.1131	1.1078
95	1.1523	1.1468	1.1412	1.1357	1.1307	1.1253	1.1201	1.1146	1.1093

Standard uncertainty in the temperature, $u(T)$, is 0.01 K; Standard uncertainty in the pressure, $u(p)$, is 0.01 MPa; Combined Standard uncertainty in the density $u_c(\rho)$, is 0.0001 g.cm^{-3} .

Table A5. Density as function of pressure and temperature for the [Ch]Cl + EG mixture with 3:7 molar ratio.

$\rho / \text{g.cm}^{-3}$									
p / MPa	T / K								
	283	293	303	313	323	333	343	353	363
0.1	1.1237	1.1178	1.1120	1.1061	1.1001	1.0939	1.0879	1.0820	1.0759
1	1.1241	1.1181	1.1123	1.1063	1.1004	1.0942	1.0882	1.0823	1.0764
2	1.1244	1.1184	1.1125	1.1067	1.1008	1.0948	1.0886	1.0828	1.0768
5	1.1254	1.1195	1.1136	1.1077	1.1019	1.0959	1.0898	1.0839	1.0779
7	1.1261	1.1194	1.1143	1.1085	1.1026	1.0967	1.0905	1.0847	1.0787
10	1.1271	1.1212	1.1154	1.1096	1.1036	1.0977	1.0916	1.0858	1.0798
12	1.1287	1.1228	1.1170	1.1113	1.1054	1.0995	1.0935	1.0876	1.0818
16	1.1303	1.1245	1.1187	1.1129	1.1071	1.1011	1.0952	1.0895	1.0837
20	1.1319	1.1260	1.1203	1.1147	1.1089	1.1030	1.0970	1.0913	1.0855
25	1.1335	1.1293	1.1220	1.1163	1.1105	1.1047	1.0989	1.0931	1.0873
30	1.1350	1.1308	1.1237	1.1179	1.1122	1.1062	1.1007	1.0949	1.0892
35	1.1366	1.1277	1.1253	1.1194	1.1139	1.1080	1.1024	1.0967	1.0910
40	1.1381	1.1324	1.1269	1.1212	1.1156	1.1097	1.1039	1.0984	1.0926
45	1.1395	1.1339	1.1284	1.1227	1.1172	1.1112	1.1057	1.1000	1.0943
50	1.1412	1.1354	1.1299	1.1243	1.1188	1.1130	1.1072	1.1016	1.0961
55	1.1426	1.1370	1.1314	1.1259	1.1204	1.1146	1.1089	1.1034	1.0978
60	1.1440	1.1385	1.1329	1.1275	1.1219	1.1145	1.1104	1.1050	1.0994
65	1.1454	1.1399	1.1344	1.1290	1.1236	1.1163	1.1122	1.1067	1.1011
70	1.1470	1.1399	1.1358	1.1290	1.1249	1.1177	1.1138	1.1083	1.1028
75	1.1484	1.1414	1.1358	1.1304	1.1265	1.1194	1.1153	1.1099	1.1044
80	1.1497	1.1428	1.1374	1.1319	1.1280	1.1209	1.1169	1.1116	1.1061
85	1.1512	1.1442	1.1388	1.1334	1.1295	1.1224	1.1184	1.1131	1.1076
90	1.1525	1.1456	1.1403	1.1348	1.1309	1.1240	1.1200	1.1147	1.1092
95	1.1563	1.1470	1.1417	1.1362	1.1406	1.1253	1.1238	1.1182	1.1127

Standard uncertainty in the temperature, $u(T)$, is 0.01 K; Standard uncertainty in the pressure, $u(p)$, is 0.01 MPa; Combined Standard uncertainty in the density $u_c(\rho)$, is 0.0001 g.cm^{-3} .

Table A6. Density as function of temperature for the Urea + EG mixture, at atmospheric pressure.

Urea + EG	
T / K	$\text{g}\cdot\text{cm}^{-3}$
373	1.1119
368	1.1156
363	1.1195
358	1.1234
353	1.1270
348	1.1306
343	1.1342
338	1.1378
333	1.1413
328	1.1449
323	1.1484
318	1.1519
313	1.1555
308	1.1590
303	1.1624
298	1.1659

Standard uncertainty in the temperature, $u(T)$, is 0.01 K; Combined Standard uncertainty in the density $u_c(\rho)$, is 0.0001 $\text{g}\cdot\text{cm}^{-3}$.

Viscosity

Table A7. Viscosity as function of temperature for glycerol, at 0.1 MPa.

$\eta / \text{mPa}\cdot\text{s}$			
T / K	$\eta / \text{mPa}\cdot\text{s}$	T / K	$\eta / \text{mPa}\cdot\text{s}$
313.15	297.849	395.91	7.132
318.67	205.481	401.43	6.188
324.18	144.91	406.94	5.422
329.70	104.334	412.46	4.795
335.22	76.603	417.98	4.279
340.74	57.290	423.49	3.85
346.25	43.601	429.01	3.492
351.77	33.734	434.53	3.192
357.29	26.511	440.05	2.939
362.81	21.145	445.56	2.725
368.32	17.103	451.08	2.543
373.84	14.018	456.60	2.389
379.36	11.636	462.12	2.257
384.87	9.774	467.63	2.146
390.39	8.304	473.15	2.051

Standard uncertainty in the temperature, $u(T)$, is 0.01 K; Standard uncertainty in the pressure, $u(p)$, is 0.01 MPa; Standard uncertainty in the viscosity $u(\eta)$, is 0.001 mPa·s

Table A8. Viscosity as function of temperature and pressure for [Ch]Cl + Urea eutectic mixture.

$\eta / \text{mPa}\cdot\text{s}$				
p / MPa	T / K			
	373	353	333	313
0.1	14.900	30.260	74.170	27.640
1	15.960	30.380	74.540	29.870
5	15.940	31.170	75.440	30.590
12	16.530	32.080	79.150	31.720
20	17.080	33.340	83.500	32.930
40	18.560	37.050	95.360	35.870
60	20.230	40.930	106.140	39.580
80	22.140	44.710	121.530	-
100	23.950	46.720	146.350	43.390

Standard uncertainty in the temperature, $u(T)$, is 0.01 K; Standard uncertainty in the pressure, $u(p)$, is 0.01 MPa; Standard uncertainty in the viscosity $u(\eta)$, is 0.001 mPa·s.

Table A9. Viscosity as function of temperature and pressure for the [Ch]Cl + Gly eutectic mixture.

$\eta / \text{mPa}\cdot\text{s}$				
p/MPa	T/K			
	373	353	333	313
0.1	17.050	31.600	65.530	165.670
1	17.260	31.830	65.060	169.840
3	-	31.850	66.710	-
5	17.750	31.870	67.680	173.610
10	-	32.830	-	-
20	18.460	34.250	72.750	189.320
40	20.350	37.610	81.690	212.360
60	22.130	41.390	90.950	238.870
80	23.760	45.230	101.270	270.220
100	25.960	49.240	110.890	305.020

Standard uncertainty in the temperature, $u(T)$, is 0.01 K; Standard uncertainty in the pressure, $u(p)$, is 0.01 MPa; Standard uncertainty in the viscosity $u(\eta)$, is 0.001 mPa·s.

Table A10. Boiling temperatures as function of ethylene glycol mole fraction for the Urea + EG mixture, at 0.07 MPa.

T/K	x_{EG}
457.40	1.00
458.70	0.96
459.41	0.93
459.90	0.91
460.34	0.89
460.78	0.89
460.72	0.91
461.53	0.87
461.77	0.85
462.24	0.85
464.45	0.84
465.42	0.81
466.18	0.81
466.73	0.80
466.51	0.82
467.77	0.79

Standard uncertainty in the temperature, $u(T)$, is 0.01 K; Standard uncertainty in the pressure, $u(p)$, is 0.01 MPa; Standard uncertainty in the composition $u(x_{\text{EG}})$, is 0.01

Table A 11 Boiling temperatures as function of the composition of ethylene glycol for the Urea + EG mixture, at 0.1 MPa.

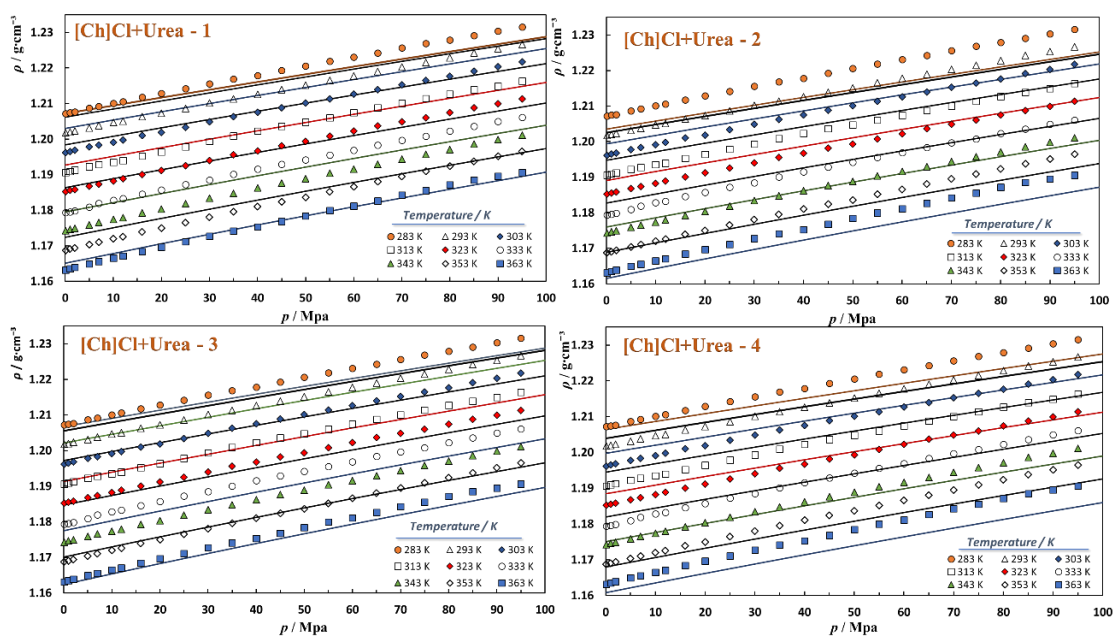
T/K	x_{EG}
469.57	0.99
470.78	0.93
471.14	0.92
471.68	0.92
471.94	0.90
472.35	0.89
472.75	0.88
472.76	0.88
473.42	0.87
473.86	0.87
473.29	0.87
474.27	0.86
474.00	0.85
474.25	0.85
474.37	0.85
474.65	0.83
476.13	0.83
475.90	0.82
476.65	0.81
476.86	0.80
476.56	0.80
477.45	0.79
478.01	0.79
477.71	0.78
478.12	0.78
478.20	0.78
478.75	0.76
478.79	0.76
478.54	0.75
478.97	0.74
479.42	0.72
480.02	0.71
479.89	0.70
480.98	0.69

Standard uncertainty in the temperature, $u(T)$, is 0.01 K; Standard uncertainty in the temperature, $u(p)$, is 0.01; ; Standard uncertainty in the composition $u(x_{EG})$, is 0.001 .

Appendix B – soft-SAFT EoS optimization

Table B.1. Urea soft-SAFT EoS molecular parameters for the optimization attempts.

Urea	Attempts			
	1	2	3	4
m	2.709	2.654	2.925	2.831
σ (Å)	3.084	3.079	3.011	3.041
ε/k_B (K)	421.9851	392.648	408.474	439.968
$\varepsilon^{HB}/k_B - 1$ (K)	1695.000	1695.000	1695.000	1695.00
$\varepsilon^{HB}/k_B - 2$ (K)	2218.335	679.705	3317.561	2006.873
$k^{HB} - 1$ (Å ³)	2000.00	2000.00	2000.00	2000.00
$k^{HB} - 2$ (Å ³)	2000.00	2000.00	2000.00	2000.00
η	0.982	0.984	0.982	0.983
ζ	1	1	1.1	1

**Figure B.1.** Density as a function of temperature and pressure, for the choline chloride with urea mixture. The solid lines represent the soft-SAFT description.

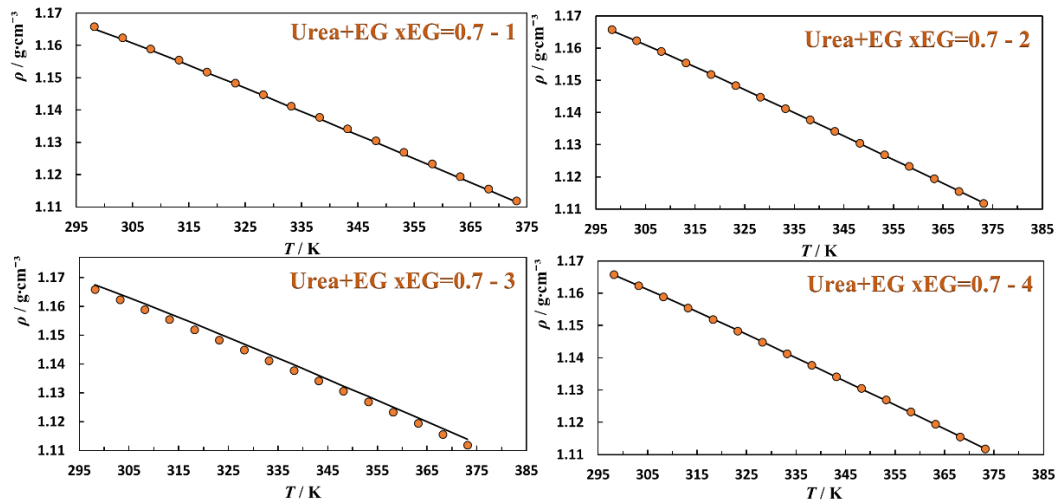


Figure B.2. Density as a function of temperature for the mixture Urea with ethylene glycol, at atmospheric pressure. The solid lines represent the soft-SAFT description.

Table B.2. soft-SAFT EoS viscosity parameters tested for ethylene glycol.

EG	Attempts				
	1	2	3	4	5
α (J·m ³ /mol·kg)	137.93	139.36	396.37	196.00	212.67
B	0.01	0.01	0.002	0.006	0.005
L_v (Å)	0.12	0.13	0.039	0.081	0.074

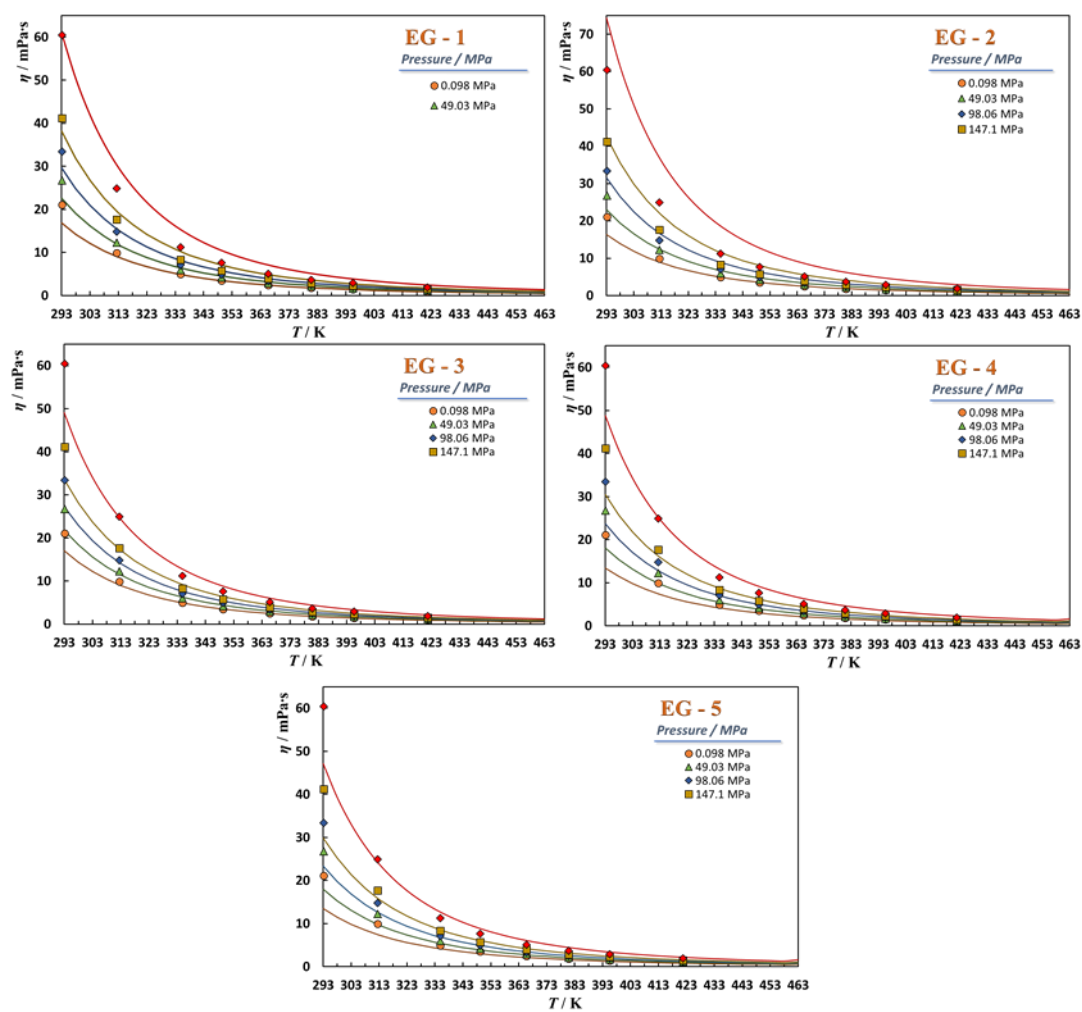


Figure B.3. Viscosity as a function of temperature and pressure for the ethylene glycol. The solid lines represent the soft-SAFT description.

Table B.3. soft-SAFT EoS viscosity parameters tested for glycerol.

α ($\text{J}\cdot\text{m}^3/\text{mol}\cdot\text{kg}$)	122.8325
B	0.025863
L_v (\AA)	0.003658

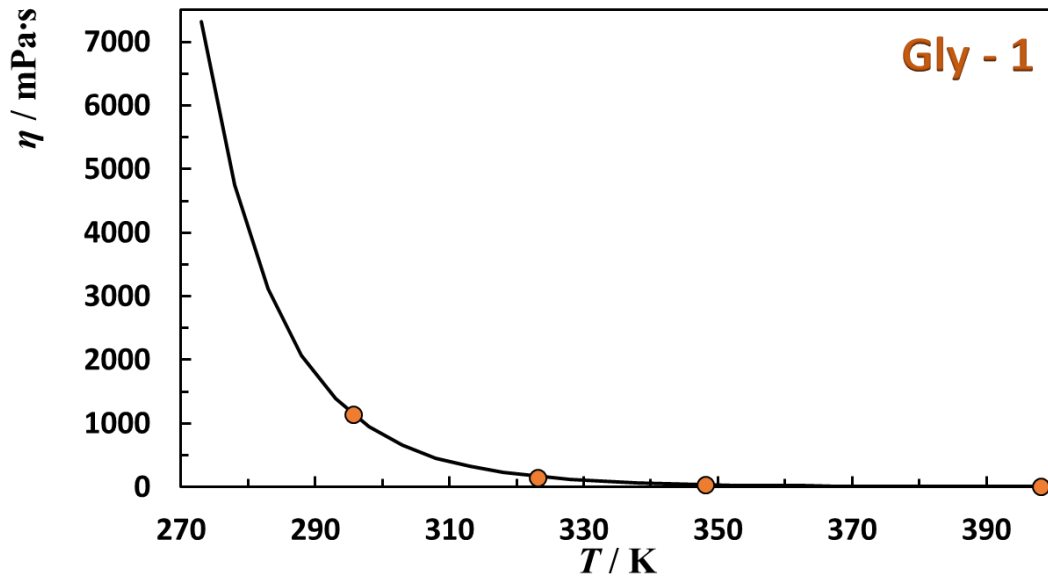


Figure B.4. Viscosity as a function of temperature for the glycerol, at atmospheric pressure. The solid lines represent the soft-SAFT description.

Table B.4. soft-SAFT EoS viscosity parameters tested for choline chloride.

[Ch]Cl	Attempt							
	1	2	3	4	5	6	7	8
α	91.05	190.62	19.69	91.05	33.85	17.43	19.07	135
$B \cdot 10^{-2}$	$2.89 \cdot 10^{-2}$	$2.47 \cdot 10^{-2}$	$6.08 \cdot 10^{-2}$	$2.81 \cdot 10^{-2}$	$6.15 \cdot 10^{-2}$	$4.87 \cdot 10^{-2}$	$5.88 \cdot 10^{-2}$	$2.22 \cdot 10^{-2}$
$L_v \cdot 10^{-3}$	$5.60 \cdot 10^{-3}$	$5.72 \cdot 10^{-3}$	$1.00 \cdot 10^{-3}$	$1.22 \cdot 10^{-3}$	$5.99 \cdot 10^{-4}$	$9.26 \cdot 10^{-4}$	$3.48 \cdot 10^{-4}$	$4.58 \cdot 10^{-4}$

In the table **Table B.4** the units of the soft-SAFT parameters are $\text{J} \cdot \text{m}^3 / \text{mol} \cdot \text{kg}$ for α , B is adimensional and L_v is in \AA

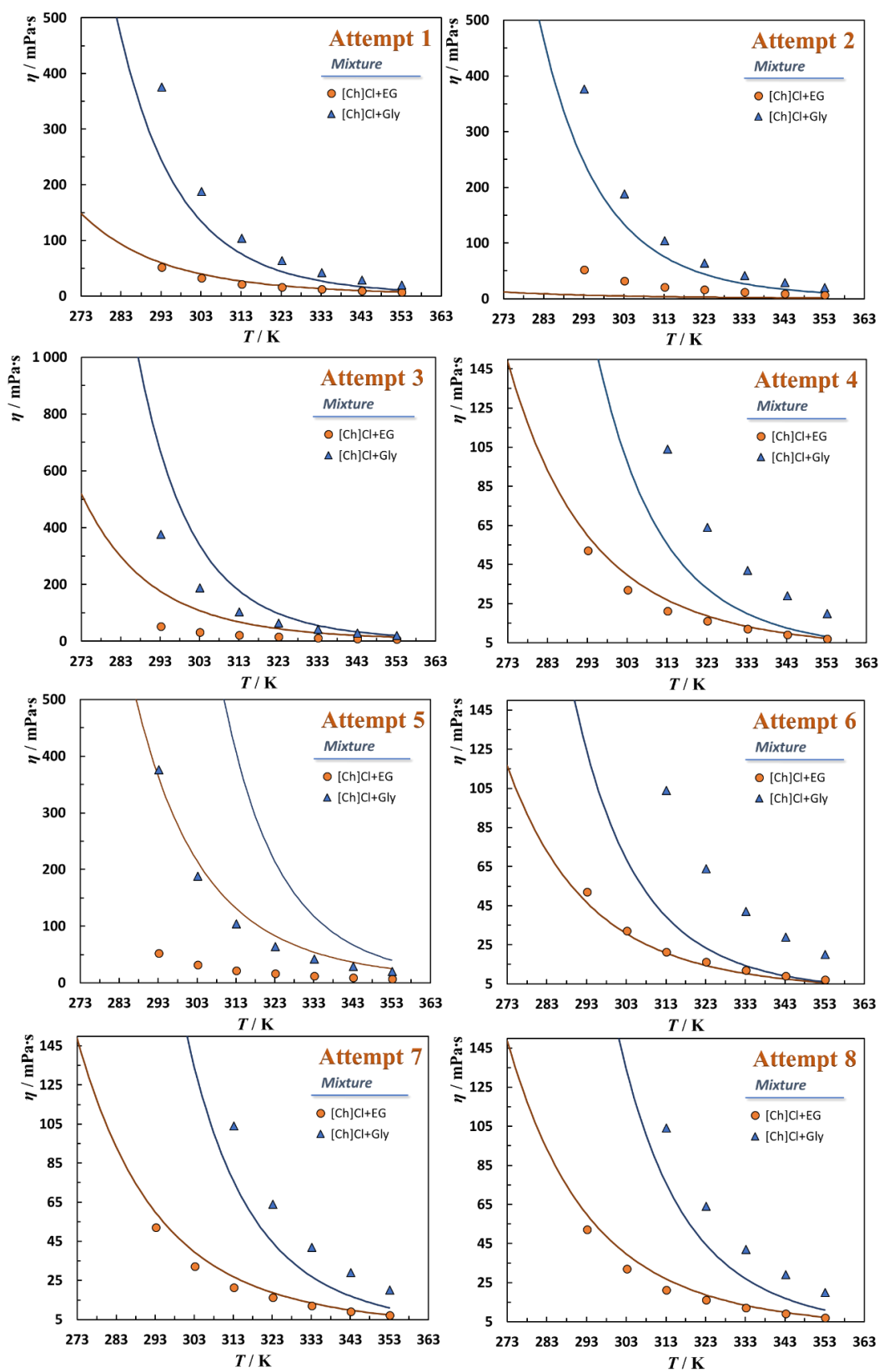


Figure B.5. Viscosity as a function of temperature for the eutectic mixture of choline chloride with ethylene glycol and with glycerol, at atmospheric pressure. The solid lines represent the soft-SAFT description.

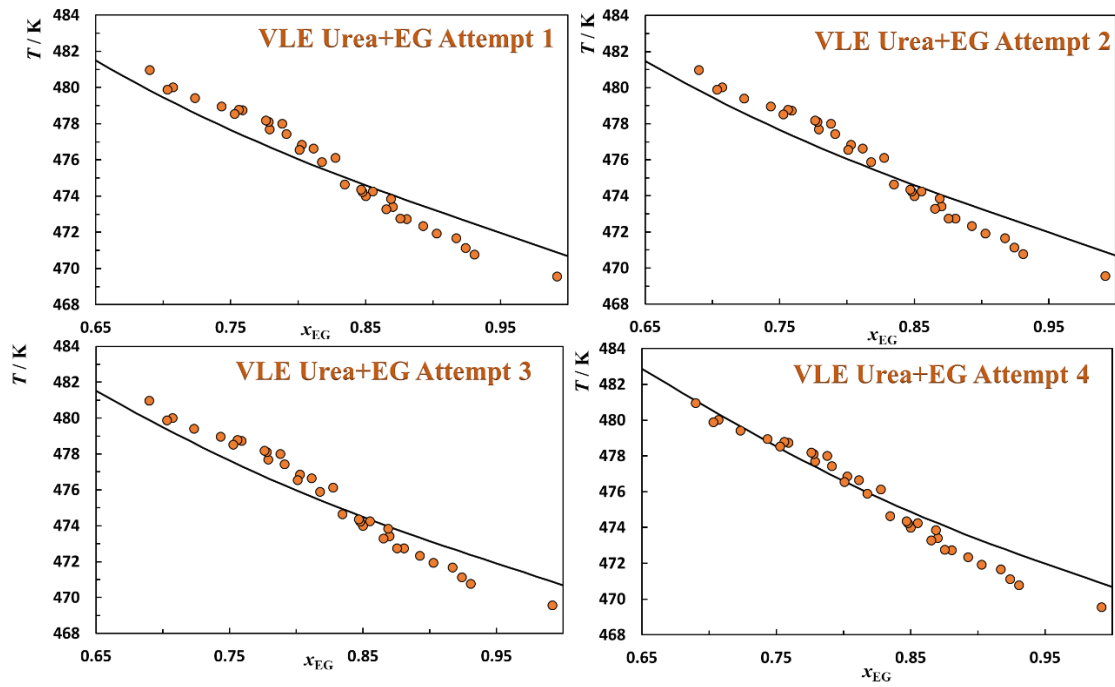


Figure B.6. Boiling temperatures in function of ethylene glycol mole fraction for the mixture urea with ethylene glycol, at atmospheric pressure. The solid line is the soft-SAFT description.

Table B.5. Molecular and cross-association parameters of the various attempts.

Urea	1	2	3	4
Number of Segments (m)	2.70	2.70	2.65	2.74
Segment diameter (σ)	3.083	3.08	3.07	3.07
Dispersive energy (ε/k_B)	421.98	421.98	392.6483	420.38
Cross-association ($\varepsilon^{\text{HB}}/k_B$)	2218.33	2218.33	679.70	2255.19